

**BGD**

10, 5923–5975, 2013

**PFTs and Export  
Production  
1960–2006**

C. Laufkötter et al.

This discussion paper is/has been under review for the journal Biogeosciences (BG).  
Please refer to the corresponding final paper in BG if available.

# Long-term trends in ocean plankton production and particle export between 1960–2006

**C. Laufkötter, M. Vogt, and N. Gruber**

Environmental Physics, Institute of Biogeochemistry and Pollutant Dynamics, ETH Zürich, Zürich, Switzerland

Received: 22 December 2012 – Accepted: 11 March 2013 – Published: 27 March 2013

Correspondence to: C. Laufkötter (charlotte.laufkoetter@env.ethz.ch)

Published by Copernicus Publications on behalf of the European Geosciences Union.

Title Page

Abstract

Introduction

Conclusions

References

Tables

Figures



Back

Close

Full Screen / Esc

Printer-friendly Version

Interactive Discussion



## Abstract

We analyse long-term trends in marine primary and particle export production and their link to marine phytoplankton community composition over the period 1950–2006 using a hindcast simulation of the ocean component of the Community Climate System Model to which the Biogeochemical Elemental Cycling Model had been coupled. In our simulation, global primary and export production decreased by 6 % and 7 %, respectively over the last 50 yr. These changes go along with a 8 % decrease in small phytoplankton biomass and 5 % decrease in zooplankton biomass. Diatom biomass decreases by 3 % with strong temporal and spatial variability. Strongest decreases in primary and export production occurred in the Western Pacific, where increased stratification leads to a decrease in total phytoplankton and a decrease in diatom fraction. This causes decreases in zooplankton biomass and a lower export efficiency. Strong phytoplankton composition changes occur in the Southern Ocean and North Atlantic, where increased wind stress leads to stronger mixing, which reduces the biomass of small phytoplankton, while diatoms profit from higher nutrient inputs and lower grazing pressure. The relative fraction of diatoms correlates positively with the export efficiency ( $r = 0.8$ ) in most areas except the Northern Pacific and Antarctic Circumpolar Current, where the correlation is negative ( $r = -0.5$ ). However, long-term trends in global export efficiency are ultimately driven by decreases in small phytoplankton and consequent decreases in coccolithophore biomass.

## 1 Introduction

In the last decades, evidence for impacts of climate change on the global oceans has been accumulating (Denman et al., 2007). The ocean surface has warmed by  $0.2^{\circ}\text{C}$  per decade in the last 30 yr (Levitus et al., 2009). Warmer surface water increases ocean stratification and reduced the mixing of the surface waters with the nutrient-rich deeper waters. Consequently, the oligotrophic areas in the Atlantic and Pacific ocean

BGD

10, 5923–5975, 2013

## PFTs and Export Production 1960–2006

C. Laufkötter et al.

Title Page

Abstract

Introduction

Conclusions

References

Tables

Figures

◀

▶

◀

▶

Back

Close

Full Screen / Esc

Printer-friendly Version

Interactive Discussion



have increased by 15 % over the period 1998 to 2006 (Polovina et al., 2008). In addition, ocean acidification has been changing the chemical composition of seawater since the onset of the industrial revolution lead to vastly increased emissions of CO<sub>2</sub> into the atmosphere. Compared to preindustrial times, the ocean pH at present has decreased by 0.1 units. This is assumed to be the strongest modification of oceanic pH in the past hundreds of thousands of years (Pelejero et al., 2010). These physical and chemical changes might have affected marine ecosystems and marine productivity already in a substantial manner, but very little is known so far about how marine plankton has changed in the last 50 yr.

Marine plankton are an important player in the global carbon cycle. Marine phytoplankton take up carbon in the surface ocean during growth. Zooplankton excretion and aggregation transform the biologically bound carbon into particles that sink into the ocean interior. This process is known as the biological pump (Volk and Hoffert, 1985). Different types of plankton have been classified into functional groups (PFTs), which play specific roles in global biogeochemical cycles and show varying effectiveness in transporting carbon to the ocean interior (Iglesias-Rodríguez, 2002; Le Quéré et al., 2005). In addition to changes in total primary production, changes in plankton community structure might influence export production.

Estimating the response of the biological pump to the anthropogenic disturbance of the global climate is still challenging. It is expected that in nutrient-limited areas with little vertical mixing and shallow mixed layer depths, climate induced stratification leads to stronger nutrient limitation. Therefore productivity and consequently export production is projected to decrease (Steinacher et al., 2009). Conversely, in light-limited areas with strong mixing and deep mixed layer depths, stratification may lead to reduced light limitation and enhanced productivity and export production (Doney et al., 2006). This relation between productivity and stratification has been confirmed in satellite-based measurements for the 1997–2006 period (Behrenfeld et al., 2006) and in models simulating future climate change (Steinacher et al., 2009). However, little is known on how primary and export production may have already changed in the past decades.

## PFTs and Export Production 1960–2006

C. Laufkötter et al.

[Title Page](#)[Abstract](#)[Introduction](#)[Conclusions](#)[References](#)[Tables](#)[Figures](#)[Back](#)[Close](#)[Full Screen / Esc](#)[Printer-friendly Version](#)[Interactive Discussion](#)

## PFTs and Export Production 1960–2006

C. Laufkötter et al.

Title Page

Abstract

Introduction

Conclusions

References

Tables

Figures



Back

Close

Full Screen / Esc

Printer-friendly Version

Interactive Discussion



Observed changes in marine ecosystems are for instance the earlier onset of the spring bloom (Sommer and Lengfellner, 2008), the expansion of warm-water species into intermediate waters (Barnard et al., 2004; Beaugrand et al., 2002) or alterations of the plankton community structure in regional ecosystems (Alheit and Niquen, 2004; Beaugrand, 2004; Richardson and Schoeman, 2004). Recently, Boyce et al. (2010) estimated trends in global chlorophyll concentration for the last century, reporting an overall decline in marine plankton biomass of approximately 1 % of the global median per year. However, these trends have been controversially discussed (Rykaczewski and Dunne, 2011; Mackas, 2011; McQuatters-Gollop et al., 2011). The current knowledge regarding changes in plankton community structure is even more limited. Researchers try to estimate the present distribution of PFTs (Alvain et al., 2008; Hirata et al., 2011; Buitenhuis et al., 2012) and to reproduce their distribution in climate models (Aumont, 2003; Kishi et al., 2007; Gregg and Casey, 2007; Buitenhuis et al., 2010). Increases in stratification are assumed to favor small phytoplankton species against larger diatoms, and decreases in diatom fraction in turn might lead to less efficient export of organic matter (Marinov et al., 2010; Bopp et al., 2005).

Modeling studies can help to uncover trends in net primary production (NPP), export production and PFT distribution that have already occurred. In this work we analyse the influence of climate change on the biological pump in a hindcast from 1960–2006. We focus on the mechanisms influencing changes in biomass, community structure and the fate of organic carbon on regional and global scale. We describe the simulated changes in export production and analyse the changes in plankton community structure and their drivers. We investigate the relationship between changes in community structure and the efficiency of export production and we describe changes in the way how carbon is routed from PFT biomass to sinking particles.

## 2 Material and methods

### 2.1 Model description

We use simulations from the Biogeochemical Elemental Cycling model BEC (Moore et al., 2002, 2004; Doney et al., 2006) embedded in the ocean component (Parallel Ocean Program) of the global climate model CCSM3 (Collins et al., 2006). The spatial resolution is  $3.6^\circ$  in longitude and  $0.8$  to  $1.8^\circ$  in latitude, with a finer resolution around the equator (Yeager et al., 2006). The ocean component of the CCSM3 has 25 vertical levels with increasing thickness from approximately 12 to 450 m. The ecosystem model BEC models biomass and chlorophyll content of four plankton functional types (PFTs), one zooplankton functional type and three phytoplankton types: diatoms, diazotrophs and a small phytoplankton class, which represents nano- and picoplankton and includes an implicit representation of calcifiers. The diazotrophs are limited by  $\text{PO}_4^{3-}$  (phosphate), Fe (iron) and light, while all other considered phytoplankton functional types are also limited by  $\text{NH}_4^+$  (ammonia) and  $\text{NO}_3^-$  (nitrate). Finally, diatoms are also limited by  $\text{Si(OH)}_4$  (silicic acid). Nutrients and light are co-limiting, with the nutrient limitation with regard to a nutrient  $n$  being calculated according to a Michaelis-Menten nutrient uptake kinetics. The total nutrient limitation is then set as the minimum limitation factor of all nutrients. Light limitation is calculated according to Geider et al. (1998), temperature sensitivity is calculated with the  $Q_{10}$  temperature function Eppley (1972) and is identical for all plankton types. Diatom and small phytoplankton growth is calculated as a maximum growth rate which is then modified according to nutrient, temperature and light availability. Phytoplankton C/N/P ratios are fixed, while the Fe/C, Si/C and Chl/C ratios are variable and depend on nutrient and light availability. Diatom uptake of silicic acid and production of  $\text{SiO}_2$  increases under iron stress and is reduced under silicate stress. The coccolithophore fraction and  $\text{CaCO}_3$  production is a function of temperature and nutrient concentrations and is also dependent on biomass levels of the small phytoplankton.

BGD

10, 5923–5975, 2013

PFTs and Export  
Production  
1960–2006

C. Laufkötter et al.

Title Page

Abstract

Introduction

Conclusions

References

Tables

Figures

◀

▶

◀

▶

Back

Close

Full Screen / Esc

Printer-friendly Version

Interactive Discussion



The phytoplankton compartments are grazed by one zooplankton class, which is parameterized to represent micro- and mesozooplankton. Depending on the type of prey, zooplankton has a variable growth rate and the routing of grazed organic matter to the detrital pools is weighted differently.

5 Of particular relevance for our work are the formation and sinking of particulate organic carbon (POC). Two detrital pools are modeled, one consisting of dissolved organic matter (DOM) and the other consisting of particulate organic matter (POM). Particulate organic matter is mainly produced by zooplankton grazing and by diatoms and small phytoplankton via aggregation. A small fraction of POC production ( $\ll 1\%$ ) is  
10 generated by non-grazing mortality of diatoms, small phytoplankton and zooplankton. Cell aggregation losses of phytoplankton are calculated using a quadratic function of biomass. Therefore, aggregation losses are low at low biomass levels but increase significantly under bloom conditions. Particles formed during grazing are calculated as a fraction of grazed matter, depending on PFT type. If diatoms are the food source,  
15 a constant fraction (26%) of the grazed carbon is routed to the POM pool. If small phytoplankton are the food source, the fraction that is routed into POC depends on the calcifier fraction and in addition increases linearly with increasing biomass, to represent a stronger microbial loop at low biomass levels. The carbon associated with  $\text{CaCO}_3$  is assumed to form sinking particles and is always routed to the POC pool. As an upper  
20 limit, not more than 22% of the grazed small phytoplankton can be routed to POC. As the fraction of grazed matter is temperature dependent, the fraction of grazed matter that forms sinking particles is (indirectly) temperature dependent, too, while aggregation depends only on biomass. The diazotrophs do not produce POC via aggregation and also zooplankton does not produce POC when grazing on diazotrophs. In addition  
25 diazotrophs constitute only a very small fraction of total phytoplankton (Moore et al., 2002). As this work deals with the influence of plankton functional types on particle export production, the analysis of the ecosystem model in this work is restricted to diatoms, small phytoplankton and zooplankton.

---

## PFTs and Export Production 1960–2006

C. Laufkötter et al.

---

[Title Page](#)[Abstract](#)[Introduction](#)[Conclusions](#)[References](#)[Tables](#)[Figures](#)[Back](#)[Close](#)[Full Screen / Esc](#)[Printer-friendly Version](#)[Interactive Discussion](#)

## PFTs and Export Production 1960–2006

C. Laufkötter et al.

Title Page

Abstract

Introduction

Conclusions

References

Tables

Figures

◀

▶

◀

▶

Back

Close

Full Screen / Esc

Printer-friendly Version

Interactive Discussion



POC instantly sinks and remineralizes in the same grid cell where it originates. Sinking and remineralization is modeled according to the mineral ballast model by Armstrong et al. (2002). Particles can be ballasted with  $\text{CaCO}_3$ ,  $\text{SiO}_2$  or mineral dust, each of which has different dissolution length scales and protect a different fraction of organic carbon from remineralization. Parameters for the ballast materials are based on the sediment trap analysis of Klaas and Archer (2002). Phytoplankton types influence the sinking behaviour of organic matter through the production of  $\text{SiO}_2$  (diatoms) and  $\text{CaCO}_3$  (small phytoplankton).

The formulas and parameters describing phytoplankton growth, grazing, export production and sinking of particles are given in the Appendix.

## 2.2 Forcing

The CCSM3 was forced with the CORE CIAF version 2 (Common Ocean-Ice Reference Experiments Corrected Inter-Annual Forcing), which was calculated using the NCEP reanalysis dataset (Kalnay et al., 1996) and satellite based estimates of radiation, sea surface temperature, sea-ice concentration and precipitation (Large and Yeager, 2009). The simulations include a 3000 yr preindustrial spin-up simulation forced with climatological means from the same forcing data followed by a transient simulation for the 1950–2006 period. We do not consider the first 10 yr of the transient simulation, to account for the change in forcing, resulting in 47 yr of model data for analysis, i.e., from January 1960 through Dec 2006. Biomass and export changes in a control run forced with constant climate are of the order of 0.1 %.

## 2.3 Model evaluation

An extensive evaluation of the BEC coupled to the CCSM was done by Doney et al. (2009b). The evaluation focused on time-mean spatial patterns, seasonal cycle and interannual variability of several ecological variables, among others chlorophyll, NPP and surface nutrients. The datasets used for comparison have been taken from Conkright

## PFTs and Export Production 1960–2006

C. Laufkötter et al.

Title Page

Abstract

Introduction

Conclusions

References

Tables

Figures



Back

Close

Full Screen / Esc

Printer-friendly Version

Interactive Discussion



et al. (2001) for surface nutrients and from McClain et al. (2004) for SeaWIFS surface chlorophyll. Integrated primary production has been calculated using SeaWIFS data and the VGPM model (Behrenfeld and Falkowski, 1997). We give a brief summary of the evaluation results and refer to Doney et al. (2009b) for more details. In contrast to our simulation they used the CORE-IAF version 1 forcing (Large and Yeager, 2004). Moreover, some parameters of the BEC have been modified, a list with the differences can be found in the Table 1.

Doney et al. (2009b) showed that the global mean bias of NPP and chlorophyll is relatively small. Surface chlorophyll tends to be overestimated in the subtropical oligotrophic gyres and underestimated in the subpolar gyres. The model-data correlation of spatial variation in the long-term mean is relatively low ( $r < 0.4$ ), the model-data correlations for the seasonal anomalies are between 0.3 and 0.7. The correlation of NPP with annual mean vertical profiles is larger than 0.95, but 0.56 for chlorophyll, mostly because the model simulates the deep chlorophyll maximum at a too shallow depth. Interannual variability is well captured in the low latitudes, but not as good in the mid- and high-latitude regions. The model skill in reproducing sea surface temperature and surface nutrient fields is consistently higher across most of the metrics than for the simulated ecological fields, and is intermediate for surface  $p\text{CO}_2$ ,  $\text{CO}_2$  and  $\text{O}_2$  air-sea fluxes.

Recently, the representation of PFTs in the CCSM-BEC has been compared to satellite-based estimates of PFT distribution (Alvain et al., 2008; Hirata et al., 2011), measurements of PFT distribution (Buitenhuis et al., 2006, 2010) and to other ecosystem models in Hashioka et al. (2012); Sailley et al. (submitted) and Vogt et al. (in prep). The diatom fraction at the peak timing of blooms varies between about 20 % (Alvain et al., 2008) and 70 % (Hirata et al., 2011) in satellite-based estimates. The CCSM-BEC results are closer to the Hirata et al. (2011) estimate with high diatom fraction (> 80 %) at peak timing of bloom (Hashioka et al., 2012). In the annual mean, the location of regions in which diatoms dominate biomass are captured by the BEC. However, the extent of these regions is overestimated in the BEC compared to results of Alvain

et al. (2008) and Hirata et al. (2011) (Vogt et al., in prep). Since the BEC simulates a generic zooplankton type, comparison to data or other models is unfeasible. However, the modelled generic zooplankton mostly resembles the microzooplankton class of other models (Sailley et al., submitted).

5 In our simulation, average global NPP is  $4.8 \text{ Pg C yr}^{-1}$  in the satellite-covered period (1998–2006), which is comparable with estimates from 24 satellite algorithms ( $50.7 \text{ Pg C yr}^{-1}$  on average) (Carr et al., 2006). NPP varies strongly with season ( $3.3$ – $4.6 \text{ Pg C month}^{-1}$ ), which is in a similar range as the estimate of Behrenfeld et al. (2006) ( $3.8$ – $4.6 \text{ Pg C month}^{-1}$ ). Global estimates for mean annual particle export production  
10 are between  $9.7$ – $12 \text{ Pg C yr}^{-1}$  using satellite-based estimates (Gnanadesikan, 2004) and  $9.8 \text{ Pg C yr}^{-1}$  using inverse estimates (Schlitzer, 2002). Najjar et al. (2007) report  $13 \pm 3 \text{ Pg C yr}^{-1}$  across 75 m as average of 12 global ocean models which use the same biogeochemical model. Our estimates vary between  $6.5$  and  $7.3 \text{ Pg C yr}^{-1}$  across the nearest depth level (80 m). While the focus in this work is on particle export production,  
15 we recognize the importance of DOC to total export production. In our simulation, between  $0.9$  and  $1.1 \text{ Gt DOC yr}^{-1}$  are exported through the 80 m level. The total export production (DOC and POC) is between  $7.4$ – $8.4 \text{ Pg C yr}^{-1}$ . This is significantly lower than estimates of other climate models ( $17 \pm 6 \text{ Pg C yr}^{-1}$ , Najjar et al., 2007).

## 2.4 Calculation of trends

20 Trends have been calculated for each grid cell using a linear regression. Significance of trends has been tested with a  $t$  test ( $\alpha = 0.5$ ). Degrees of freedom have been reduced when performing the  $t$  test as described in, e.g. Zwiers and von Storch (1995) to account for autocorrelation. Changes in percent were obtained by normalising all results to the mean of the first ten years.

25 Particle export production (EP) is defined as the average POC flux through the 100 m depth level for each year. NPP is given as annual mean vertically integrated net primary production between surface and 100 m depth. Phytoplankton and zooplankton biomass are given as annual mean average concentration between surface and 100 m depth.

## BGD

10, 5923–5975, 2013

### PFTs and Export Production 1960–2006

C. Laufkötter et al.

Title Page

Abstract

Introduction

Conclusions

References

Tables

Figures



Back

Close

Full Screen / Esc

Printer-friendly Version

Interactive Discussion



Export efficiency is the fraction of NPP that is exported through the 100 m depth level, i.e. EP divided by NPP. Diatom fraction is the fraction of diatom biomass compared to total phytoplankton biomass, i.e. diatom fraction = diatoms/(diatoms + small phytoplankton + diazotrophs).

### 3 Results

Our model simulation shows a significant decrease in global particle export production by  $-0.8 \text{ Gt POC yr}^{-1}$  ( $-8\%$ ) from 1960–2006, but with strong temporal and regional variability (Figs. 1 and 2c). Strongest decreases occur in the Western Subtropical Pacific ( $-2 \text{ mol POC m}^{-2} \text{ yr}^{-1}$  resp.  $-40\%$ ) and in the Subpolar Southern Ocean ( $-0.8 \text{ mol POC m}^{-2} \text{ yr}^{-1}$  resp.  $-10\%$ ) (Fig. 2c). Export production increases in the North Atlantic ( $+0.6 \text{ mol POC m}^{-2} \text{ yr}^{-1}$  resp.  $+30\%$ ) and in the Polar Southern Ocean  $> 60^\circ \text{ S}$  ( $+0.4 \text{ mol POC m}^{-2} \text{ yr}^{-1}$  resp.  $+10\%$ ). All other areas display changes of less than 5%. The trends are linear and persist also for the period from 1979 onward, where satellite observations could be used to build the forcing fields. The only exception is the Southern Ocean where export decreases again at the end of the simulation period. The magnitude of decline is greater than the interannual variability, moreover the trends are observable in all seasons and are most pronounced in autumn (September–November).

Changes in simulated net primary production are strongly correlated with the changes in export production (spatial Spearman correlation  $S_c = 0.96$ ). However, changes in NPP are between 2–20% weaker than changes in EP. The amplification of trends between NPP and export is caused by changes in export efficiency (Fig. 1c). Changes in export efficiency are strongly correlated with changes in export production ( $S_c = 0.88$ ) and also NPP (Figs. 1 and 2). As a result, the trends in export are amplified strongest in areas where the largest changes in NPP occur, i.e. the Western Subtropical Pacific, North and Equatorial Atlantic and the Southern Ocean.

BGD

10, 5923–5975, 2013

## PFTs and Export Production 1960–2006

C. Laufkötter et al.

Title Page

Abstract

Introduction

Conclusions

References

Tables

Figures

◀

▶

◀

▶

Back

Close

Full Screen / Esc

Printer-friendly Version

Interactive Discussion



NPP (and EP) changes are negatively correlated with changes in SST (Fig. 3) in the low latitudes but positively correlated in the high latitudes. In the tropics the decrease of NPP with increasing SST is strongest, while increase of NPP with increasing SST in the Southern Ocean is rather weak (not shown).

5 The simulated changes in NPP and EP are associated with extensive shifts in diatom NPP and small phytoplankton NPP (Fig. 4). Globally, diatom NPP decreases by  $-3\%$ . In the North Atlantic and the Southern Ocean, diatom net primary production increases between  $+30\%$  and  $+60\%$ , except in the area west of the Antarctic Peninsula ( $120^\circ$  to  $80^\circ$  W,  $50^\circ$  to  $70^\circ$  S), where diatom NPP decreases ( $-30\%$ ). In the Equatorial and  
10 Western Pacific, in particular in the subtropical gyres, diatom NPP decreases by almost  $60\%$  over the 1960 to 2006 period. Diatom biomass distribution changes correlate positively with diatom NPP changes ( $S_c = 0.87$ ), with increases in the high latitudes and decreases in the low latitudes.

Small phytoplankton NPP shows strongly contrasting trends to diatom NPP in the  
15 high latitudes but similar changes in the low latitudes (Fig. 4a, b). The global average decrease of small phytoplankton NPP is  $-8\%$ . The model simulates strong decreases in small phytoplankton NPP in the Southern Ocean ( $-45\%$ ), except for the area west of the Antarctic Peninsula where small phytoplankton NPP increases. In almost all other areas small phytoplankton biomass decreases between  $-2\%$  and  $-40\%$ , with  
20 strongest decreases in the subtropical gyres, North and Equatorial Atlantic. Trends in small phytoplankton biomass follow trends in small phytoplankton NPP ( $S_c = 0.84$ ), but in the Equatorial Pacific small phytoplankton NPP decreases whereas small phytoplankton biomass increases). As a consequence of the changes in diatom and small phytoplankton NPP, the diatom fraction substantially increases in the North Atlantic and the Southern Ocean by up to  $40\%$ , except the area west of the Antarctic Peninsula  
25 where diatom fraction decreases. The diatom fraction also decreases in the Equatorial and Subtropical Pacific, in particular in the western part ( $-20\%$ ,  $-50\%$ ). Zooplankton biomass follows changes in small phytoplankton NPP almost everywhere (Fig. 4), but zooplankton changes are weaker than changes in small phytoplankton NPP.

---

**PFTs and Export  
Production  
1960–2006**C. Laufkötter et al.

---

[Title Page](#)[Abstract](#)[Introduction](#)[Conclusions](#)[References](#)[Tables](#)[Figures](#)[Back](#)[Close](#)[Full Screen / Esc](#)[Printer-friendly Version](#)[Interactive Discussion](#)

The production of  $\text{SiO}_2$  follows the trends in diatom fraction ( $S_c = 0.77$ ), as can be expected from the fact that only diatoms produce  $\text{SiO}_2$ . Changes in  $\text{SiO}_2$  production caused by differences in Si/C ratio of diatoms account for about 5% of the total changes in  $\text{SiO}_2$  production.  $\text{CaCO}_3$  is produced by the calcifying fraction of small phytoplankton and depends on small phytoplankton biomass, temperature and nutrient limitation. The simulated temperature changes have little influence on  $\text{CaCO}_3$  production. Trends in  $\text{CaCO}_3$  production therefore follow trends in small phytoplankton biomass, but they are amplified in regions where nutrient limitation increases, e.g. the Tropical Pacific. As  $\text{CaCO}_3$  is only produced by small phytoplankton, the rain ratio is strongly negatively correlated to the diatom fraction ( $S_c = -0.81$ ). Consequently, the rain ratio shows significant changes where the phytoplankton community composition changes strongly, i.e. in the Southern Ocean, North Atlantic and Western Pacific.

## 4 Discussion

### 4.1 What mechanisms drive PFT distribution, export and export efficiency?

Phytoplankton biomass and PFT distribution is controlled by a complex interplay between bottom-up processes (changes in nutrient and light availability) and top-down processes (changes in grazing pressure). In a steady-state system (constant biomass), there is a balance between nutrient and light supply on the one hand and grazing by zooplankton on the other hand. In a non-steady-state system, trends in biomass can be caused by changes in nutrients or light availability, in which case we call it a bottom-up controlled trend, or it can be caused by changes in grazing pressure, in which case we call it a top-down controlled trend.

While in the real ocean changes in zooplankton biomass are influenced by a variety of factors like, e.g. the presence of larger predators or direct effects of climate change on the zooplankton life cycle and resulting phenological mismatches (Edwards and Richardson, 2004), zooplankton biomass in the model depends only on temperature,

**BGD**

10, 5923–5975, 2013

## PFTs and Export Production 1960–2006

C. Laufkötter et al.

Title Page

Abstract

Introduction

Conclusions

References

Tables

Figures



Back

Close

Full Screen / Esc

Printer-friendly Version

Interactive Discussion



phytoplankton biomass and zooplankton biomass. Of these variables, temperature is the only one which can be directly affected by climate change. Strong changes in temperature are needed to significantly alter the total grazing pressure as well as the relative grazing fraction on different prey. As the mean temperature change in our simulation period is 0.3 °C on global average, the resulting changes in grazing pressure drive about 5 % of the observed trends. Therefore, we conclude that trends in our simulation are mostly bottom-up controlled. However, once phytoplankton biomass starts changing, zooplankton grazing adapts, leading to a change in the relative grazing pressure on the different phytoplankton PFTs ( $p$  PFTs) in some regions. The grazing pressure strongly contributes to the dominance of diatoms, see also Hashioka et al. (2012); Sailley et al. (submitted). Therefore, the magnitude of change in  $p$  PFT biomass as well as PFT composition is adjusted by zooplankton grazing.

#### 4.1.1 Physical changes

The model simulates a warming of 0.5 to 1.5 °C of the surface ocean in the low and mid latitudes (cooling in the North Pacific and Southern Ocean of about -1 °C). The mean global increase in SST is +0.3 °C, which is slightly below the estimate by Smith et al. (2008) (+0.4 °C). Salinity increases in the North Atlantic (+0.8 units) and in the southern part of the Tropical Pacific (+1), and decreases in the northern part of the Tropical Pacific (-1.0 units). Warming and salinity changes cause an increase in stratification in the low latitudes and a decrease in stratification in the Southern Ocean and North Atlantic. The forcing fields used for this simulation prescribe increases in wind stress, particularly in the Southern Ocean and North Atlantic, and weaker winds in the Tropical Pacific. As a consequence of changes in wind and stratification, the simulated MLD deepens in the North Atlantic and Southern Ocean by up to 40 %. In the Equatorial Pacific, MLD shoaled substantially (-40 %). The changes in stratification and MLD affect phytoplankton directly by changing the light availability and have strong effects on nutrient supply, with nutrient concentrations generally increasing where stronger mixing occurs and vice versa.

**BGD**

10, 5923–5975, 2013

### PFTs and Export Production 1960–2006

C. Laufkötter et al.

Title Page

Abstract

Introduction

Conclusions

References

Tables

Figures

◀

▶

◀

▶

Back

Close

Full Screen / Esc

Printer-friendly Version

Interactive Discussion



## 4.1.2 Effect of physical changes on NPP and PFT composition

The consequence of the altered light and nutrient supply are substantial changes in both light and nutrient limitation, which are shown in Fig. 5 (map of changes) and Fig. 2b (timeseries for selected regions).

5 The general pattern is one of increased light availability but higher nutrient stress in the low latitudes, and decreased light availability but lower nutrient stress in the high latitudes, for both phytoplankton types. The effect is a substantial decrease of NPP in both regimes.

Temperature changes have only a weak oh phytoplankton growth effect compared to changes in nutrients and light. Warming in the surface ocean slightly increases NPP, but this effect is compensated by decreases in NPP caused by decreased nutrient and light availability. The mechanisms we find confirm the findings of several authors, e.g. (Doney et al., 2007), and are in accordance with several climate model studies analysing climate change in the next century (Steinacher et al., 2009; Bopp et al., 2001; Boyd and Doney, 2002; Sarmiento et al., 2004; Le Quéré et al., 2003).

While the general pattern in nutrient and light changes is similar for diatoms and small phytoplankton, the magnitude of growth limitation is different for the two PFTs. Diatom and small phytoplankton growth is calculated with a multiplicative growth function where the growth rate  $\mu$  of phytoplankton group  $x$  calculated as follows:

$$20 \mu_x = \mu_{\max} \times T_f \times N_x \cdot L_x, \quad (1)$$

where  $\mu_{\max}$  denotes the maximum growth rate for diatoms and small phytoplankton and  $T_f$ ,  $N_x$  and  $L_x$  are temperature, nutrient and light limitation (see Appendix).

Small phytoplankton are parameterized to have lower nutrient requirements, they aren't silicate limited and they have higher light requirements. The diatoms in contrast are better adapted to low light, high nutrient regimes. Temperature affects both  $p$  PFTs equally and therefore cannot be the cause for differences in growth rates of  $p$  PFTs. An illustration for the (resulting) difference in growth rate of diatoms and small phytoplankton at different iron/nitrate and light levels is shown in Fig. 6.

**BGD**

10, 5923–5975, 2013

### PFTs and Export Production 1960–2006

C. Laufkötter et al.

Title Page

Abstract

Introduction

Conclusions

References

Tables

Figures

◀

▶

◀

▶

Back

Close

Full Screen / Esc

Printer-friendly Version

Interactive Discussion



Fig. 5 shows the changes in the product of nutrient and light limitation for both diatoms and small phytoplankton. With the help of the limitation factors, most trends can be explained. The Tropical Pacific is a regime where small phytoplankton have a significant advantage in growth compared to diatoms (Fig. 6). The warming of the surface ocean, increased stratification and lower wind stress lead to higher nutrient stress for both  $p$  PFTs and reduce the growth rate of both  $p$  PFTs. In addition, the difference in growth rate between diatoms and small phytoplankton becomes larger, i.e. the growth rate of the diatoms decreases more strongly than that of the small phytoplankton. Therefore the PFT composition shifts towards lower a diatom fraction.

Under the conditions typical for the Southern Ocean and North Atlantic (high nutrient concentration but little light availability), small phytoplankton have only a weak advantage in growth compared to diatoms. During the last 50 yr, both regions underwent an increase in wind stress, which further strengthens light-limitation and further weakens nutrient-limitation. In the Southern Ocean, the growth rate of both  $p$  PFTs is reduced, but the difference in growth rate becomes smaller with time, i.e. diatoms and small phytoplankton have a more similar growth rate at the end of the simulation. Considering only bottom-up factors we would expect the PFT composition to shift towards similar amounts of diatoms and small phytoplankton, as they have a similar growth rate. In the North Atlantic only small phytoplankton growth is reduced, while diatom growth accelerates, in accordance with changes in their limitation factors. We conclude that the changes in total phytoplankton and also phytoplankton composition can be at first order explained with the changes in limitation factors. However, Fig. 6 shows that small phytoplankton always have a higher growth rate than diatoms under typical occurring nutrient and light values. Considering only bottom-up factors, one would expect small phytoplankton to always dominate biomass. In addition, not all trends can be explained exclusively by the growth limitation factors, e.g. diatom biomass increases although the limitation stays rather constant in the Southern Ocean. This indicates that grazing pressure is of importance in understanding changes in phytoplankton biomass.

## BGD

10, 5923–5975, 2013

### PFTs and Export Production 1960–2006

C. Laufkötter et al.

Title Page

Abstract

Introduction

Conclusions

References

Tables

Figures



Back

Close

Full Screen / Esc

Printer-friendly Version

Interactive Discussion



### 4.1.3 Zooplankton grazing and bottom-up vs. top-down control

Grazing on phytoplankton type  $x$  is calculated according to a Holling type III functional response (Holling, 1965). Grazing has the same temperature dependence as phytoplankton growth. The maximal zooplankton growth rate is higher for small phytoplankton than for diatoms. Therefore, zooplankton biomass is strongly coupled to small phytoplankton biomass and closely follows trends in small phytoplankton PP ( $S_c = 0.79$ , Figs. 4, 7).

The observed changes in temperature only have a weak effect on zooplankton grazing. Changes in zooplankton grazing are at first order triggered by changes in phytoplankton biomass. The consequential change in zooplankton biomass amplifies the changes in grazing pressure. Therefore trends in  $\rho$  PFT biomass are initiated by changes in bottom-up factors and are then modified by changes in zooplankton grazing.

To illustrate the response of grazing pressure to changing phytoplankton biomass, we analyse the specific grazing rate  $SG(P_x)$ , which is the grazing rate  $G(P_x)$  on phytoplankton  $P_x$ , normalized by zooplankton concentration  $Z$  (Hashioka et al., 2012):

$$SG(P_x) = \frac{G(P_x)}{Z} = u_{P_x}^{\max} \cdot T_f \cdot \left( \frac{P_x^2}{P_x^2 + g_x^2} \right), \quad (2)$$

where  $u_{P_x}^{\max}$  is the maximum grazing rate,  $T_f$  the temperature dependence and  $g_x$  a zooplankton grazing coefficient, see Table 1 and Appendix. Figure 6 shows the difference in specific grazing rate in dependence of the prey biomass ratio. At equal biomass, small phytoplankton experience a higher grazing pressure than diatoms. This difference in grazing pressure becomes larger at higher biomass levels.

The higher grazing pressure of zooplankton on small phytoplankton partly balances the advantage in growth rate of small phytoplankton and makes it possible for diatoms to dominate biomass in regions where their growth rate is close to the growth rate of small phytoplankton, i.e. in high nutrient low light regimes. This top-down control

of phytoplankton composition in the BEC has also been analysed in Hashioka et al. (2012).

In the Tropical Pacific, changes in light- and nutrient-limitation lead to decreases in small phytoplankton biomass and stronger decreases in diatom biomass. Consequently, zooplankton biomass also decreases. The effect is less grazing of both  $p$  PFTs, and little changes in the difference in grazing pressure (Fig. 6). Trends in the Tropical Pacific are therefore only weakly modified by top-down processes. In the North Atlantic, changes in nutrient and light availability lead to increases in diatom biomass while small phytoplankton biomass changes only slightly. This shift in biomass ratio leads to a stronger relative grazing on diatoms. Trends in the North Atlantic are therefore weakened by top-down processes.

In the Southern Ocean, small phytoplankton biomass decreases because of changes in light and nutrient limitation, while for diatoms decreases in light limitation are compensated by increases in nutrient limitation. The decrease in small phytoplankton is accompanied by a decrease in zooplankton biomass. Zooplankton doesn't follow the increase in total phytoplankton in the Southern Ocean, as the increase in total biomass is associated with a strong shift towards more diatoms and zooplankton growth rates are lower when feeding on diatoms.

The changes in PFT composition in the Southern Ocean shift the specific grazing pressure towards a stronger diatom grazing. But as zooplankton biomass decreases, the total grazing pressure decreases. This decreases total grazing pressure and allows diatom biomass to increase.

In summary, trends in PFT composition can mostly be explained by changes in light and nutrient availability. Temperature induced changes in zooplankton grazing explain only a small fraction of the simulated phytoplankton biomass changes.

Changes in top-down control which have been caused by changes in phytoplankton biomass weaken phytoplankton trends in the high latitudes, but top-down control has little influence on trends in the low latitudes. Therefore we identify bottom-up processes as the primary driver of the changes.

**PFTs and Export  
Production  
1960–2006**

C. Laufkötter et al.

Title Page

Abstract

Introduction

Conclusions

References

Tables

Figures



Back

Close

Full Screen / Esc

Printer-friendly Version

Interactive Discussion



In order to understand how the changes in PFT composition are connected to the amplification of EP compared to NPP we analyse the pathways along which carbon is routed from PFT biomass to sinking particles.

#### 4.1.4 Carbon pathways from PFT biomass to sinking particles

5 In the BEC, particles are formed through four different pathways. These are zooplankton grazing of diatoms or small phytoplankton and via aggregation by either small phytoplankton or diatoms. Figure 8 shows which of these four pathways of POC formation is the most important for the longterm mean in our simulation. In the low and mid latitudes, the production of particles is dominated by grazing on small phytoplankton (55% of total POC), with only small exceptions. The reason is that small phytoplankton dominate biomass in the low and mid latitudes, and grazing pressure is amplified by high temperatures. Aggregation in the low and mid latitudes is less relevant as biomass is kept low due to grazing.

15 In the high latitudes, diatom aggregation contributes the highest carbon flux to the sinking particle pool (54% of total POC in Southern Ocean originates from diatom aggregation). In these regions, the diatom fraction is high and grazing pressure is low because of the cold temperatures. Biomass reaches high levels, which results in significant aggregation fluxes. Small phytoplankton aggregation dominates particle formation in areas where small phytoplankton has a high biomass and a high fraction of calcifiers. Grazing on diatoms dominates POC production only in few localized areas (Fig. 8).

20 The dominance pattern shown in Fig. 8 shows only little change over time. During 50 yr of simulation, regions where POC production is dominated by small phytoplankton aggregation have decreased (-4%) in favour of regions where diatom aggregation dominates POC production (not shown).

25 However, substantial changes in the magnitude of the four fluxes occur on regional scales. Trends for the regions in which export production changed most are shown in Fig. 9. In the Southern Ocean (Fig. 9a), diatom aggregation increased by 11% compared to the beginning of the simulation, to the disadvantage of the grazing fluxes.

BGD

10, 5923–5975, 2013

### PFTs and Export Production 1960–2006

C. Laufkötter et al.

Title Page

Abstract

Introduction

Conclusions

References

Tables

Figures

◀

▶

◀

▶

Back

Close

Full Screen / Esc

Printer-friendly Version

Interactive Discussion



This reflects increases in diatom biomass and decreases in small phytoplankton and zooplankton. In the tropical Pacific (Fig. 9b), all fluxes decrease by about 20 %. In the North Atlantic (Fig. 9c) both diatom related fluxes increase while small phytoplankton fluxes show little changes.

#### 4.1.5 Relation between particle production mechanism and export efficiency

Increases in diatom fraction lead to a higher fraction of particles ballasted with  $\text{SiO}_2$  and a stronger particle production during grazing. Consequently, the diatom fraction is strongly positively correlated with the export efficiency almost everywhere in our simulation (Spearman correlation coefficient  $> 0.8$ ), Fig. 10). However, there is one notably exception: at about  $50^\circ \text{S}$  and around  $50^\circ \text{N}$  in the Pacific, the correlation is significantly negative (Spearman correlation coefficient between  $-0.8$  and  $-1$ ).

In those areas, two factors influence the export efficiency of small phytoplankton: First, small phytoplankton include a high coccolithophore fraction, which leads to a strong production of  $\text{CaCO}_3$ .  $\text{CaCO}_3$  is parameterized to be a more effective ballasting material than silicate (following Klaas and Archer, 2002), therefore causing a higher export efficiency. Second, aggregation is parameterized to depend exponentially on biomass in our model. A decrease in small phytoplankton at a high biomass level causes a stronger reduction in particle production than an increase in diatoms at a low biomass level can compensate for.

A third factor influencing export efficiency in our model is the biomass level of small phytoplankton. At low biomass levels, small phytoplankton is assumed to be composed of nano/picophytoplankton species. The fraction of grazed matter that is routed to POC is parameterized to be smaller to reflect a stronger microbial loop. Hence, a decrease in small phytoplankton biomass leads to a lower export efficiency. In our simulation this effect dominates in the low latitudes, where diatom biomass is very low and grazing on small phytoplankton constitutes the most important particle export flux.

In summary, export efficiency (Fig. 1e and f) decreases strongly in the low latitudes, because of both a lower diatom fraction and decreases in small phytoplankton biomass.

BGD

10, 5923–5975, 2013

## PFTs and Export Production 1960–2006

C. Laufkötter et al.

Title Page

Abstract

Introduction

Conclusions

References

Tables

Figures

◀

▶

◀

▶

Back

Close

Full Screen / Esc

Printer-friendly Version

Interactive Discussion



Export efficiency increases in the North Atlantic driven by a higher diatom fraction. In the area south of 30° S, the diatom fraction increases, but small phytoplankton biomass and coccolithophore fraction decreases strongly, causing an overall decrease in export efficiency. On the global scale, diatom fraction increases but export efficiency decreases (Fig. 2d).

## 4.2 Comparison to model studies and measurements for the 1950–2006 time period

### 4.2.1 Long-term measurements of Chl and NPP

In a recent study, Boyce et al. (2010) compiled chlorophyll and transparency measurements to estimate global trends in chlorophyll since 1899. They report decreases in chlorophyll in eight out of ten ocean regions and a global rate of decline of 1 % of the global median per year.

The Boyce et al. (2010) paper has been discussed controversially in the community. One major point of critic was the statistical handling of the combination of transparency and chlorophyll measurements (Rykaczewski and Dunne, 2011; Mackas, 2011). Hence, for comparison with our simulation time period, we can the transparency measurements and use chlorophyll measurements only. In our simulation we also find a global decline in chlorophyll, with an overall reduction in chlorophyll biomass of 5 % over the simulation period. Our hindcast is able to reproduce the direction of in situ chlorophyll trends for the 1960–2006 period described in Boyce et al. (2010) in the Equatorial Atlantic and Pacific, Northern Indian Ocean, Southern Ocean, i.e. in about half of the regions. However, our simulated trends differ in several other regions. In particular, in the North Atlantic our simulation shows a strong increase in chlorophyll. Furthermore, Boyce et al. (2010) report increases in chlorophyll in the North Pacific, South Indian and South Pacific, where our simulation shows decreases (North and South Pacific) or no clear trend (South Indian).

BGD

10, 5923–5975, 2013

## PFTs and Export Production 1960–2006

C. Laufkötter et al.

Title Page

Abstract

Introduction

Conclusions

References

Tables

Figures

◀

▶

◀

▶

Back

Close

Full Screen / Esc

Printer-friendly Version

Interactive Discussion



## PFTs and Export Production 1960–2006

C. Laufkötter et al.

Title Page

Abstract

Introduction

Conclusions

References

Tables

Figures



Back

Close

Full Screen / Esc

Printer-friendly Version

Interactive Discussion



McQuatters-Gollop et al. (2011) pointed out that the results from Boyce et al. (2010) contradict results from several long-term measurements. First, the dataset collected by the Continuous Plankton Recorder survey (CPR, Edwards, 2001) shows an increase in the Phytoplankton Colour Index in both the Northeast and Northwest Atlantic basins (Edwards, 2001; Head and Pepin, 2010; Reid et al., 1998; Raitos, 2005; McQuatters-Gollop et al., 2007), which is in good agreement with our simulated trends. Second, the Hawaii Ocean Time-series (HOT), the Bermuda Atlantic Time Series (BATS) and the California Cooperative Oceanic Fisheries Investigations (CalCOFI) also indicate increases in phytoplankton NPP for the tropical North Atlantic and tropical East Pacific. (Saba et al., 2010; Kahru et al., 2009). Saba et al. (2010) report an average increase in NPP of 2 % per year for the 1989–2007 period at both HOT and BATS station. According to our simulation, both HOT and BATS are located in regions where rather weak or insignificant trends occur over the full simulation period. However, for the 1989–2007 period our simulation shows an increase in Chl and NPP at HOT of 15 %, but a decrease of about 5 % at BATS. Finally, the number of measurements on which Boyce et al. (2010) based their trends are sparse in general and extremely low in the southern hemisphere, where our trends differ most from their results. At the moment it is not possible to distinguish whether the model has weaknesses in reproducing trends in the southern hemisphere, or if the observational record is not strong enough to derive reliable trends.

In summary, our trends are comparable to several long-term chlorophyll and NPP measurements. Moreover we can reproduce the direction of the trends reported by Boyce et al. (2010) in the Equatorial Atlantic and Pacific, Northern Indian Ocean and Southern Ocean.

### 4.2.2 Satellite based estimates of Chl and NPP

Several authors gave satellite-based estimates for global inventory of chlorophyll and NPP and for trends over the satellite-covered period (Gregg, 2003; Antoine, 2005; Behrenfeld et al., 2006). Behrenfeld et al. (2006) report a significant increase from

1997–1999 of 0.3 Tg chlorophyll, followed by a decrease of 0.1 Tg yr<sup>-1</sup> until 2006. Moreover, their estimated NPP changes are highly correlated with changes in stratification in the permanently stratified oceans ( $r^2 = 0.73$ ).

Our simulation does not show a significant trend in total chlorophyll over the SeaWiFS period. However, changes in NPP are highly correlated to changes in SST (Spearman correlation = -0.81) during the 1997–2006 period, and this correlation also exists throughout the 1960–2006 period (Spearman correlation -0.87, see also Fig. 3). The link between stratification and NPP is strongest in the low latitudes. In the Southern Ocean the correlation between stratification and NPP is very weak (0.04).

Gregg (2003) used re-analyzed, blended satellite-in situ chlorophyll data records of Coastal Zone Color Scanner (CZCS) and SeaWiFS data to estimate changes in global ocean primary production from the early-to-mid 1980's to the present. They report a decline in NPP of more than 6 % since the early 1980's, with nearly 70 % of the global decline occurring in the high latitudes. On the other hand, Antoine (2005) applied revised algorithms to the CZCS data as well as the first 5 yr of SeaWiFS data to produce an internally consistent time-series. Results show an increase in global chlorophyll of about 22 %, mainly due to large increases in the tropical areas and to a lesser extent increases in the higher latitudes. Oligotrophic gyres display declining concentrations.

Our simulation shows no significant decrease in global mean chlorophyll between the two satellite-covered periods. We find significant decreases in most of the oligotrophic gyres (-15 %) and both regions of significant increase and decrease in the intermediate and high latitudes. However, the interannual variability in the simulation is strong, making it difficult to detect significant trends in the satellite-covered time period. Satellite observations on longer time scales are needed for better evaluation of climate models.

**BGD**

10, 5923–5975, 2013

## PFTs and Export Production 1960–2006

C. Laufkötter et al.

Title Page

Abstract

Introduction

Conclusions

References

Tables

Figures

⏪

⏩

◀

▶

Back

Close

Full Screen / Esc

Printer-friendly Version

Interactive Discussion



### 4.2.3 Model studies

While there are many model studies examining primary and export production under future climate change (Steinacher et al., 2009; Bopp et al., 2001; Boyd and Doney, 2002; Sarmiento et al., 2004; Bopp et al., 2005), there are only few studies analysing hindcasts of the past 50 yr.

Wang and Moore (2012) did an analysis of NPP and export production in the Southern Ocean from 1979–2003 in a hindcast, using a modified version of the BEC which includes Prochlorococcus as a new PFT. Their model was forced with the NCEP reanalysis data (Large and Yeager, 2009) and ice fraction satellite data published in Large and Yeager (2004). As we are using an earlier version of the same model, our results are very close to findings of Wang and Moore (2012). Analog to our results, they report decreasing trends in sinking POC and NPP for the Southern Ocean ( $> 30^{\circ}$  S), caused by changing mixed layer depths and iron concentrations. Their mean annual NPP south of  $30^{\circ}$  S is slightly lower than in our simulation ( $12.4 \text{ Pg C yr}^{-1}$  vs.  $13 \text{ Pg C yr}^{-1}$  between 1997 and 2003 and for the region south of  $50^{\circ}$  S  $2.7 \text{ Pg C yr}^{-1}$  vs.  $3.5 \text{ Pg C yr}^{-1}$ ). However, both our results and results given by Wang and Moore (2012) are within range of previous estimates (e.g. Arrigo et al., 1998; Carr et al., 2006; Moore and Abbott, 2000).

Furthermore, Steinacher et al. (2009) analyse the evolution of NPP and export production in three fully-coupled climate models for the period from 1860 until 2099. The models are forced with reconstructed  $\text{CO}_2$  and from 2000 onwards with the SRES A2 scenario. They report a coherent decline in NPP and export between 7 and 20% at the end of the century compared to preindustrial conditions. The trends are not linear but show little changes until about 1950 and exponentially decreased afterwards. Changes in NPP in the 1960–2010 period are about  $-3\%$  in these simulations. Our projected changes for the 1960–2006 period are slightly larger than the trends reported by Steinacher et al. (2009), the model shows a linear decrease of  $-6\%$  and  $-7\%$  for NPP and export production, respectively. A linear continuation of our trends

BGD

10, 5923–5975, 2013

## PFTs and Export Production 1960–2006

C. Laufkötter et al.

Title Page

Abstract

Introduction

Conclusions

References

Tables

Figures



Back

Close

Full Screen / Esc

Printer-friendly Version

Interactive Discussion



would result in  $-12\%$  NPP and  $-18\%$  export until 2100, compared to the 1960–1969 period, which is within the range given by Steinacher et al. (2009).

In summary, our trends are within the range of other model projections for the 1960–2006 period. In particular, our trends are comparable to model estimates simulating anthropogenic climate change based on CO<sub>2</sub> emissions.

### 4.3 Implications for future change

The interactions between climate change, ocean biology and export production that we describe in this study are comparable to other model studies, in particular models predicting future climate change: the negative correlation between stratification and NPP in the low latitudes (and positive correlation in the high latitudes) in our simulation is in agreement with results from satellite data (Behrenfeld et al., 2006). Several climate model studies indicate that this mechanism might also prevail during the next 100 yr (Steinacher et al., 2009; Bopp et al., 2001; Boyd and Doney, 2002; Le Quéré et al., 2003).

In addition, our results show a negative correlation between stratification and diatom fraction. This mechanism has also been found in studies that analyse future climate change in different ocean models (Marinov et al., 2010; Bopp et al., 2005). Furthermore, the effects of changes in diatom fraction on export efficiency are complex in our simulation. We find a positive correlation between interannual variability of diatom fraction and export efficiency, except in those regions with high coccolithophore fraction (Fig. 10). While this is in accordance with previous assumptions about the relationship between diatom fraction and export efficiency (Le Quéré et al., 2005), diatom fraction is not the main driver of long-term global trends in export efficiency in our simulation. Other important factors influencing export efficiency are the coccolithophore fraction and the concentration of small phytoplankton biomass, which is associated with the efficiency of the microbial loop in our model. In contrast to our results, in the study by Bopp et al. (2005) the change in diatom fraction resulted in a reduced efficiency of the biological pump on a global scale under a future  $4 \times \text{CO}_2$  scenario. Changes in export

Title Page

Abstract

Introduction

Conclusions

References

Tables

Figures



Back

Close

Full Screen / Esc

Printer-friendly Version

Interactive Discussion



production (−25 %) have been significantly stronger than changes in NPP (−15 %) in their study.

Considering the contrasting mechanisms in our hindcast simulation compared to the mechanisms identified in the future study by Bopp et al. (2005), projections of export efficiency seem to be strongly dependent on the ecosystem representation in the model. Further model studies are needed to explore the range of possible interactions between PFT composition and export efficiency.

#### 4.4 Caveats and limitations

Important mechanisms that are not considered in our study include the effects of ocean acidification on PFT growth and on calcification rates, and a decoupling of the C : N : P ratio. These processes affect the PFT distribution and biogeochemical cycles and have previously been found to be of relevance for the export efficiency (Weber and Deutsch, 2012; Doney et al., 2009a). Including these processes into ecosystem models has been hampered by sparse availability of data of PFT distribution and behavior. The recent development of new datasets describing PFT abundance (Buitenhuis et al., 2012) and nutrient utilization traits of PFTs (Edwards et al., 2012) is an important step forward and will help model development and improve performance of ecosystem models.

The representation of the second trophic level in the BEC as one single zooplankton class seems to mostly mimic the behaviour of microzooplankton (Sailley et al., submitted), effects of mesozooplankton grazing and other higher trophic levels might be insufficiently considered in our simulation. Likewise, impacts of climate change on larger predators or on the zooplankton life cycle might exert additional changes in top-down control on phytoplankton which are not considered in our simulation. Furthermore, the model assumes the same temperature sensitivity for phytoplankton growth and for zooplankton grazing. Heterotrophic processes have been assumed to show stronger responses to elevated temperatures (Pomeroy and Wiebe, 2001; Riebesell et al., 2009) than NPP. We need further research to better understand the balance between NPP and grazing processes under increasing temperatures (Riebesell et al., 2009).

**BGD**

10, 5923–5975, 2013

### PFTs and Export Production 1960–2006

C. Laufkötter et al.

Title Page

Abstract

Introduction

Conclusions

References

Tables

Figures

◀

▶

◀

▶

Back

Close

Full Screen / Esc

Printer-friendly Version

Interactive Discussion



Finally, we focus our analysis exclusively on the particle export production. However, DOC is assumed to contribute up to 20 % of total export production (Najjar et al., 2007). Changes in DOC export are an important part of total export production and should be included in further studies to complete our picture of future export production.

## 5 Conclusions

Our results provide further support for a decline in chlorophyll, NPP and export production during the last 50 yr. The trends in our simulation are mostly driven by bottom-up controls, with decreased nutrient concentrations being the main driver in the low latitudes and increased light limitation the main driver in the higher latitudes. However, the representation of top-down control is restricted to temperature effects on grazing of one zooplankton type in our model. We have shown that a parameterization of PFTs including diatoms, coccolithophores and small phytoplankton of variable size impacts the dynamics of particle production in a non-linear way. We suggest further model studies to uncover the full range of possible responses of export efficiency to changes in PFT composition, on the basis of our current understanding of PFTs. Both better estimates of PFT distribution and measurements of the contribution of different PFTs to the particle flux are needed. New datasets of PFT biomass and pigment concentrations provide a promising step towards improved model evaluation (Buitenhuis et al., 2012). More accurate satellite-based PFT estimates will also be helpful in this regard (Alvain et al., 2008; Hirata et al., 2011). It is assumed that Climate change has been weaker in the past 50 yr but will accelerate in the upcoming century. Stronger perturbations of the marine ecosystems are likely to affect PFT distribution, primary and export production to a wider extent than shown in this work. Including improved representations of PFT distribution and behaviour in simulations of future climate change might reveal an important feedback of the biological pump to climate change.

## Appendix A

### Model equations and parameters

We give the model equations for PFT growth, grazing, particle production and sinking in the following. Model parameters are written in bold and the values are given in Table 1.

#### 5 A1 Changes in PFT biomass

The changes in biomass of a phytoplankton PFT  $P_x$  are calculated as:

$$\frac{D(P_x)}{Dt} = \mu_x \times P_x - G_x - \text{agg}_x - \text{loss}_x, \quad (\text{A1})$$

where  $\mu_x$  denotes the growth rate,  $G_x$  the loss due to grazing,  $\text{agg}_x$  the loss due to aggregation and  $\text{loss}_x$  representing the non-grazing mortality.

10 The growth rate for phytoplankton type  $x$  is calculated as:

$$\mu_x = \mu_{\max} \cdot T_f \cdot N_x \cdot L_x, \quad (\text{A2})$$

where  $\mu_{\max}$  denotes the maximum growth rate,  $T_f$  the temperature dependence and  $N_x, L_x$  represent nutrient and light limitation. The temperature sensitivity  $T_f$  is calculated as:

$$15 T_f = q_{10} \left( \frac{T - T_{\text{ref}}}{10} \right), \quad (\text{A3})$$

where  $q_{10}$  is a temperature reference factor,  $T$  temperature and  $T_{\text{ref}}$  a reference temperature (see Table 1). Nutrient limitation  $N_x$  is the minimum of the specific nutrient limitations:

$$N_x = \min\{N_x^{\text{Fe}}, N_x^{\text{P}}, N_x^{\text{NO}_3/\text{NH}_4}, N_x^{\text{SiO}_2}\}. \quad (\text{A4})$$

For  $n = \text{Fe}, \text{P}$  and  $\text{SiO}_2$ , specific nutrient limitation is calculated as:

$$N_x^n = \frac{n}{n + K_x^n}, \quad (\text{A5})$$

where  $K_x^n$  are the Michaelis-Menten half saturation coefficients. For  $\text{NO}_3$  and  $\text{NH}_4$  specific nutrient limitation is calculated as:

$$N_x^{\text{NO}_3} = \frac{\text{NO}_3/K_x^{\text{NO}_3}}{1 + (\text{NO}_3/K_x^{\text{NO}_3}) + (\text{NH}_4/K_x^{\text{NH}_4})} \quad (\text{A6})$$

and

$$N_x^{\text{NH}_4} = \frac{\text{NH}_4/K_x^{\text{NH}_4}}{1 + (\text{NO}_3/K_x^{\text{NO}_3}) + (\text{NH}_4/K_x^{\text{NH}_4})}. \quad (\text{A7})$$

The light limitation  $L_x$  is calculated according to Geider et al. (1998) as:

$$L_x = 1 - \exp\left(\frac{-\alpha \cdot \left(\frac{\text{Chl}}{\text{C}}\right)_x \cdot I_{\text{par}}}{\mu_{\text{max}} \cdot N_x \cdot T_f}\right), \quad (\text{A8})$$

where  $I_{\text{par}}$  is irradiance,  $\alpha$  is the initial slope of the photosynthesis-irradiance (P-I) curve and  $\left(\frac{\text{Chl}}{\text{C}}\right)_x$  is the chlorophyll to carbon ratio of phytoplankton  $x$ .

## A2 Grazing and changes in zooplankton biomass

The fraction of phytoplankton biomass  $P_x$  that is grazed by zooplankton  $Z$  is calculated with Holling type III function (Holling, 1965):

$$G_x(P_x) = u_x^{\text{max}} \cdot T_f \cdot Z \cdot \left(\frac{P_x^2}{P_x^2 + (g^2 \cdot f_z^x)}\right). \quad (\text{A9})$$

$u_x^{\max}$  is the maximum zooplankton growth rate on phytoplankton  $x$ ,  $g$  is a zooplankton grazing coefficient and  $f_z^x$  a scaling factor for grazing (see Table 1). The grazed fraction is partly incorporated into new zooplankton biomass, a part is remineralized and a fraction is routed to the sinking detritus pool.

5 The changes in zooplankton biomass  $Z$  are calculated as

$$\frac{D(Z)}{Dt} = \left( \sum_x i_z \times G_x(P_x) \right) - \text{loss}_Z \quad (\text{A10})$$

### A3 Formation of POC

The particulate organic carbon originates from grazing and aggregation and is calculated as:

$$10 \text{ POC}_{\text{production}} = G_{\text{diat}}^{\text{POC}} + G_{\text{small}}^{\text{POC}} + \text{agg}_{\text{diat}} + \text{agg}_{\text{small}}, \quad (\text{A11})$$

where  $G_{\text{diat}}^{\text{POC}}$  and  $G_{\text{small}}^{\text{POC}}$  are the fractions of grazed diatoms and small phytoplankton that are routed to the sinking particles and  $\text{agg}_{\text{diat}}$  and  $\text{agg}_{\text{small}}$  aggregation by diatoms and small phytoplankton.

### A4 Routing of grazed matter to POC

15 The fraction of grazed matter of phytoplankton  $x$  that is routed to POC,  $G_x^{\text{POC}}$ , is calculated as:

$$G_{\text{diat}}^{\text{POC}} = G_{\text{diat}} \times f_{\text{graz}}^{\text{diat, POC}} \quad (\text{A12})$$

and

$$G_{\text{small}}^{\text{POC}} = G_{\text{small}} \times \max \left\{ \min \left\{ \begin{array}{l} f_{\text{graz}}^{\text{CaCO}_3, \text{ POC}} \times Q_{\text{CaCO}_3} \\ f_{\text{graz}}^{\text{small, POC}} \times P_{\text{small}} \\ e_{\text{small}}^{\text{POC}} \end{array} \right\} \right\}. \quad (\text{A13})$$

5951

Title Page

Abstract

Introduction

Conclusions

References

Tables

Figures

◀

▶

◀

▶

Back

Close

Full Screen / Esc

Printer-friendly Version

Interactive Discussion



$f_{\text{graz}}^{\text{diat, POC}}$ ,  $f_{\text{graz}}^{\text{CaCO}_3, \text{ POC}}$  and  $f_{\text{graz}}^{\text{small, POC}}$  denote the fractions that are routed to POC, and  $e_{\text{small}}^{\text{POC}}$  is a small phytoplankton grazing factor (see Table 1).

## A5 Aggregation

Aggregation of phytoplankton  $x$  is calculated as:

$$5 \text{ agg}_x = \min \left( a_x^{\text{max}}, \rho_x \times (P_x)^2 \right), \quad (\text{A14})$$

where  $a_x^{\text{max}}$  and  $\rho_x$  are the maximum aggregation rate and a quadratic mortality rate of phytoplankton  $x$  (see Table 1). In addition, at least 1 % of diatom biomass aggregate and sink.

## A6 Sinking of particles

10 The POC pool is divided into two fractions, unballasted POC and ballasted POC. The POC associated with ballast sinks and remineralizes together with the associated ballast material. A fraction of the ballast ("hard" fraction) together with its associated POC is assumed to be resistant to degradation and is remineralized at the sea floor. More details can be found in Moore et al. (2004). The sinking of unballasted POC depending on depth  $z$  is calculated as:

$$15 \text{ POC}^{\text{flux}}(z) = \text{POC}_{z_0}^{\text{flux}} e^{-\frac{(z-z_0)}{\lambda_{\text{POC}}}} T_f^{\text{POC}} + \int_{z_0}^z \text{POC}^{\text{prod}} e^{-\frac{(z-z_0)}{\lambda_{\text{POC}}}} T_f^{\text{POC}} dz, \quad (\text{A15})$$

where  $z_0$  is depth at 0 and

$$T_f^{\text{POC}} = \text{POC} q_{10}^{\frac{(T+T_{K0})-(T_{\text{ref}}+T_{K0})}{10}}. \quad (\text{A16})$$

The sinking of ballasted POC depending on depth  $z$  is calculated as:

$$\text{POC}_{\text{ballast}}^{\text{flux}}(z) = \quad (\text{A17})$$

$$\begin{aligned} & \omega_{\text{PCaCO}_3} \left( \text{soft PCaCO}_3^{\text{flux}}(z) + \text{hard PCaCO}_3^{\text{flux}}(z) \right) \\ & + \omega_{\text{PSiO}_3} \left( \text{soft PSiO}_3^{\text{flux}}(z) + \text{hard PSiO}_3^{\text{flux}}(z) \right) \\ & + \omega_{\text{dust}} \left( \text{soft dust}^{\text{flux}}(z) + \text{hard dust}^{\text{flux}}(z) \right) \end{aligned}$$

where the  $\omega_{\text{PCaCO}_3}$ ,  $\omega_{\text{PSiO}_3}$ ,  $\omega_{\text{dust}}$  are mass ratios (see Table 1).

The sinking of soft mineral ballast ( $\text{soft PCaCO}_3^{\text{flux}}$ ,  $\text{soft PSiO}_3^{\text{flux}}$ ) is calculated as:

$$\text{soft PCaCO}_3^{\text{flux}}(z) = \text{soft PCaCO}_3^{\text{flux}}_{z_0} e^{\frac{-(z-z_0)}{\lambda_{\text{PCaCO}_3}}} + (1 - f_{\text{PCaCO}_3}^{\text{hard}}) \int_{z_0}^z \text{PCaCO}_3^{\text{prod}} e^{\frac{-(z-z_0)}{\lambda_{\text{PCaCO}_3}}} dz, \quad (\text{A18})$$

where  $\lambda_{\text{PCaCO}_3}$  is the remineralization length scale (see Table 1). The equivalent opal fluxes are:

$$\text{soft PSiO}_3^{\text{flux}}(z) = \text{soft PSiO}_3^{\text{flux}}_{z_0} e^{\frac{-(z-z_0)}{\lambda_{\text{PSiO}_3}}} + (1 - f_{\text{PSiO}_3}^{\text{hard}}) \int_{z_0}^z \text{PSiO}_3^{\text{prod}} e^{\frac{-(z-z_0)}{\lambda_{\text{PSiO}_3}}} dz. \quad (\text{A19})$$

The sinking of the hard fraction of opal and calcium carbonate is calculated as:

$$\text{hard PCaCO}_3^{\text{flux}}(z) = \text{hard PCaCO}_3^{\text{flux}}_{z_0} e^{\frac{-(z-z_0)}{\lambda_{\text{hard}}}} + f_{\text{PCaCO}_3}^{\text{hard}} \int_{z_0}^z \text{PCaCO}_3^{\text{prod}} dz, \quad (\text{A20})$$

and

$$\text{hard PSiO}_3^{\text{flux}}(z) = \text{hard PSiO}_3^{\text{flux}}_{z_0} e^{\frac{-(z-z_0)}{\lambda_{\text{hard}}}} + f_{\text{PSiO}_3}^{\text{hard}} \int_{z_0}^z \text{PSiO}_3^{\text{prod}} dz. \quad (\text{A21})$$

The sinking of soft and hard mineral dust is calculated as:

$$\text{soft dust}^{\text{flux}}(z) = \text{soft dust}_{z_0}^{\text{flux}} e^{-\frac{(z-z_0)}{\lambda_{\text{dust}}}} \quad (\text{A22})$$

and

$$\text{hard dust}^{\text{flux}}(z) = \text{hard dust}_{z_0}^{\text{flux}} e^{-\frac{(z-z_0)}{\lambda_{\text{hard}}}}, \quad (\text{A23})$$

5 again  $\lambda_{\text{P}_{\text{SiCO}_3}}$ ,  $\lambda_{\text{dust}}$  and  $\lambda_{\text{hard}}$  are the respective remineralization length scales (see Table 1).

## A7 CaCO<sub>3</sub> production

CaCO<sub>3</sub> is produced by a fraction of small phytoplankton. Calcification is reduced by nutrient limitation and temperatures below  $\text{CaCO}_3^T_{\text{thres1}}$  (which is 1 °C, see Table 1).  
 10 The maximal fraction of CaCO<sub>3</sub> producers is 40%:

$$\text{CaCO}_3^{\text{prod}} = \min \left\{ f_{\text{prod}}^{\text{sp, CaCO}_3} \times \mu_{\text{small}} \times P_{\text{small}} \times N_{\text{small}} \times T_{\text{CaCO}_3} 0.4 \times \mu_{\text{small}} \times P_{\text{small}}, \quad (\text{A24}) \right.$$

where the temperature dependence  $T_{\text{CaCO}_3}$  is calculated as follows:

$$T_{\text{CaCO}_3} = \begin{cases} 1 & T > \text{CaCO}_3^T_{\text{thres1}} \\ \max \left\{ \frac{T - \text{CaCO}_3^T_{\text{thres2}}}{\text{CaCO}_3^T_{\text{thres2}}}, 0 \right\} & T < \text{CaCO}_3^T_{\text{thres1}} \end{cases} \quad (\text{A25})$$

$\text{CaCO}_3^T_{\text{thres1}}$ ,  $\text{CaCO}_3^T_{\text{thres2}}$  are temperature thresholds for calcification (see Table 1).

## 15 A8 SiO<sub>3</sub> uptake by diatoms and opal production

Production of opal equals the SiO<sub>3</sub> uptake and is calculated as:

$$\text{SiO}_3^{\text{prod}} = Q_{\text{diat}}^{\text{Si}} \times \mu_{\text{diat}} \times P_{\text{diat}} \quad (\text{A26})$$

where

$$Q_{\text{diat}}^{\text{Si}} = \begin{cases} \min \left\{ \begin{array}{l} Q_{\text{diat, opt}}^{\text{Si}} \times f(Q) \\ 0.685 \end{array} \right. & \left( \text{Fe} < 2K_{\text{diat}}^{\text{Fe}} \right) \wedge \left( \text{SiO}_3 > 2K_{\text{diat}}^{\text{SiO}_3} \right) \\ \max \left\{ \begin{array}{l} \frac{Q_{\text{diat, opt}}^{\text{Si}} \times \text{SiO}_3}{2K_{\text{diat}}^{\text{SiO}_3}} \\ 0.0685 \end{array} \right. & \text{SiO}_3 < 2K_{\text{diat}}^{\text{SiO}_3} \\ Q_{\text{diat, opt}}^{\text{Si}} & \text{else,} \end{cases} \quad (\text{A27})$$

$$\text{with } f(Q) = \left( Q_{\text{diat, coef}}^{\text{Si}} \times \frac{2K_{\text{diat}}^{\text{Fe}}}{\text{Fe}} - Q_{\text{diat, coef}}^{\text{Si}} - 1 \right).$$

*Acknowledgements.* The research leading to these results has received funding from the European Community's Seventh Framework Programme (FP7 2007–2013) under grant agreement no. [238366]. MV and NG acknowledge funding by ETH Zürich. We thank Xavier Giraud and Heather Graven for kindly providing us with the output from their model simulations and Laurent Bopp for constructive comments and discussions.

## References

- Alheit, J. and Niquen, M.: Regime shifts in the Humboldt Current ecosystem, *Prog. Oceanogr.*, 60, 201–222, doi:10.1016/j.pocean.2004.02.006, 2004. 5926
- Alvain, S., Moulin, C., Dandonneau, Y., and Loisel, H.: Seasonal distribution and succession of dominant phytoplankton groups in the global ocean: A satellite view, *Global Biogeochem. Cy.*, 22, 1–15, doi:10.1029/2007GB003154, 2008. 5926, 5930, 5948
- Antoine, D., Morel, A., Gordon, H. R., Banzon, V. F., and Evans, R. H.: Bridging ocean color observations of the 1980's and 2000's in search of long-term trends, *J. Geophys. Res.*, 110, C6, doi:10.1029/2004JC002620, 2005. 5943, 5944
- Armstrong, R., Lee, C., Hedges, J., Honjo, S., and Wakeham, S.: A new, mechanistic model for organic carbon fluxes in the ocean based on the quantitative association of POC with ballast minerals, *Deep-Sea Res. Pt. II*, 49, 219–236, doi:10.1016/S0967-0645(01)00101-1, 2002. 5929

## PFTs and Export Production 1960–2006

C. Laufkötter et al.

Title Page

Abstract

Introduction

Conclusions

References

Tables

Figures

◀

▶

◀

▶

Back

Close

Full Screen / Esc

Printer-friendly Version

Interactive Discussion



- Arrigo, K. R., Worthen, D., Schnell, A., and Lizotte, M. P.: Primary production in Southern Ocean waters, *J. Geophys. Res.*, 103, 15587–15600, 1998. 5945
- Aumont, O.: An ecosystem model of the global ocean including Fe, Si, P colimitations, *Global Biogeochem. Cy.*, 17, 1060, doi:10.1029/2001GB001745, 2003. 5926
- Barnard, M. R., Batten, S. D., Beaugrand, G., Buckland, C., Conway, D. V. P., Edwards, M., Finlayson, J., Gregory, L. W., Halliday, N. C., John, A. W. G., Johns, D. G., Johnson, A. D., Jonas, T. D., Lindley, J. A., Nyman, J., Pritchard, P., Reid, P. C., Richardson, A. J., Saxby, R. E., Sidey, J., Smith, M. A., Stevens, D. P., Taylor, C. M., and Tranter, P. R. G., Walne, A. W., Wootton, M., Wotton, C. O. M., and Wright, J. C.: Continuous plankton records : Plankton atlas of the North Atlantic Ocean (1958–1999), II. Biogeographical charts, *Mar. Ecol. Prog. Ser., Supplement*, 11–75, 2004. 5926
- Beaugrand, G.: The North Sea regime shift: Evidence, causes, mechanisms and consequences, *Prog. Oceanogr.*, 60, 245–262, doi:10.1016/j.pocean.2004.02.018, 2004. 5926
- Beaugrand, G., Reid, P. C., Ibañez, F., Lindley, J. A., and Edwards, M.: Reorganization of North Atlantic marine copepod biodiversity and climate., *Science*, 296, 1692–4, doi:10.1126/science.1071329, 2002. 5926
- Behrenfeld, M. J. and Falkowski, P. G.: Photosynthetic rates derived from satellite-based chlorophyll concentration, *Limnol. Oceanogr.*, 42, 1–20, 1997. 5930
- Behrenfeld, M. J., O'Malley, R. T., Siegel, D. a., McClain, C. R., Sarmiento, J. L., Feldman, G. C., Milligan, A. J., Falkowski, P. G., Letelier, R. M., and Boss, E. S.: Climate-driven trends in contemporary ocean productivity, *Nature*, 444, 752–755, doi:10.1038/nature05317, 2006. 5925, 5931, 5943, 5946
- Bopp, L., Monfray, P., Aumont, O., Dufresne, J., Le Treut, H., Madec, G., Terray, L., and Orr, J.: Potential impact of climate change on marine export production, *Global Biogeochem. Cy.*, 15, 81–100, 2001. 5936, 5945, 5946
- Bopp, L., Aumont, O., Cadule, P., Alvain, S., and Gehlen, M.: Response of diatoms distribution to global warming and potential implications: A global model study, *Geophys. Res. Lett.*, 32, 2–5, doi:10.1029/2005GL023653, 2005. 5926, 5945, 5946, 5947
- Boyce, D. G., Lewis, M. R., and Worm, B.: Global phytoplankton decline over the past century, *Nature*, 466, 591–596, doi:10.1038/nature09268, 2010. 5926, 5942, 5943
- Boyd, P. W. and Doney, S. C.: Modelling regional responses by marine pelagic ecosystems to global climate change, *Geophys. Res. Lett.*, 29, 1–4, doi:10.1029/2001GL014130, 2002. 5936, 5945, 5946

## PFTs and Export Production 1960–2006

C. Laufkötter et al.

[Title Page](#)
[Abstract](#)
[Introduction](#)
[Conclusions](#)
[References](#)
[Tables](#)
[Figures](#)
[Back](#)
[Close](#)
[Full Screen / Esc](#)
[Printer-friendly Version](#)
[Interactive Discussion](#)


- Buitenhuis, E., Le Quéré, C., Aumont, O., Beaugrand, G., Bunker, A., Hirst, A., Ikeda, T., O'Brien, T., Piontkovski, S., and Straile, D.: Biogeochemical fluxes through mesozooplankton, *Global Biogeochem. Cy.*, 20, GB2003, doi:10.1029/2005GB002511, 2006. 5930
- Buitenhuis, E., Vogt, M., Moriarty, R., Bednarsek, N., Doney, S., Leblanc, K., Le Quere, C., Luo, Y., O'Brien, C., O'Brien, T., Peloquin, J., Schiebel, R., and Swan, C.: MAREDAT: Towards a world ocean atlas of marine ecosystem data, *Earth Syst. Sci. Data Discuss.*, 5, 1077–1106, doi:10.5194/essdd-5-1077-2012, 2012. 5926, 5947, 5948
- Buitenhuis, E. T., Rivkin, R. B., Saille, S., and Le Quéré, C.: Biogeochemical fluxes through microzooplankton, *Global Biogeochem. Cy.*, 24, doi:10.1029/2009GB003601, 2010. 5926, 5930
- Carr, M., Friedrichs, M., Schmeltz, M., Noguchiaita, M., Antoine, D., Arrigo, K., Asanuma, I., Aumont, O., Barber, R., and Behrenfeld, M.: A comparison of global estimates of marine primary production from ocean color, *Deep-Sea Res. Pt. II*, 53, 741–770, doi:10.1016/j.dsr2.2006.01.028, 2006. 5931, 5945
- Collins, W. D., Bitz, C. M., Blackmon, M. L., Bonan, G. B., Bretherton, C. S., Carton, J. A., Chang, P., Doney, S. C., Hack, J. J., Henderson, T. B., Keihl, J. T., Large, W. G., McKenna, D. S., Santer, B. D., and Smith, R. D.: The Community Climate System Model Version 3 (CCSM3), *J. Climate*, 19, 2545–2143, doi:10.1175/JCLI3761.1, 2006. 5927
- Conkright, M., Locarnini, H., Garcia, T., O'Brien, T., Boyer, C., and Stephens, J.: *World Ocean Atlas 2001: objective analyses, data statistics, and figures, documentation*, Tech. rep., National Oceanographic Data Center, Silver Spring, 2001. 5929
- Denman, K. L., Brasseur, G., Chidthaisong, A., Ciais, P., Cox, P., Dickinson, R. E., Hauglustaine, D., Heinze, C., Holland, E., Jacob, D., Lohmann, U., Ramachandran, S., Da Silva Dias, P. L., Wofsy, S. C., and Zhang, X.: Chapter 7: Couplings between changes in the climate system and biogeochemistry, in: *Climate Change 2007 The Physical Science Basis Contribution of Working Group I to the Fourth Assessment Report of the Intergovernmental Panel on Climate Change*, edited by: Solomon, S., Qin, D., Manning, M., Chen, Z., Marquis, M., Averyt, K. B., Tignor, M., and Miller, H. L., Cambridge University Press, United Kingdom and New York, NY, USA, 2007. 5924
- Doney, S. C., Lindsay, K., Fung, I., and John, J.: Natural variability in a stable, 1000-yr global coupled climate-carbon cycle simulation, *J. Climate*, 19, 3033–3054, doi:10.1175/JCLI3783.1, 2006. 5925, 5927

## PFTs and Export Production 1960–2006

C. Laufkötter et al.

Title Page

Abstract

Introduction

Conclusions

References

Tables

Figures



Back

Close

Full Screen / Esc

Printer-friendly Version

Interactive Discussion



- 5 Doney, S. C., Yeager, S., Danabasoglu, G., Large, W. G., and McWilliams, J. C.: Mechanisms governing interannual variability of upper-ocean temperature in a global ocean hindcast simulation, *J. Phys. Oceanogr.*, 37, 1918–1938, doi:10.1175/JPO3089.1, 2007. 5936
- Doney, S. C., Fabry, V. J., Feely, R. a., and Kleypas, J. a.: Ocean Acidification: The Other CO<sub>2</sub> Problem, *Ann. Rev. Mar. Sci.*, 1, 169–192, doi:10.1146/annurev.marine.010908.163834, 2009a. 5947
- 10 Doney, S. C., Lima, I., Moore, J. K., Lindsay, K., Behrenfeld, M. J., Westberry, T. K., Mahowald, N., Glover, D. M., and Takahashi, T.: Skill metrics for confronting global upper ocean ecosystem-biogeochemistry models against field and remote sensing data, *J. Mar. Syst.*, 76, 95–112, doi:10.1016/j.jmarsys.2008.05.015, 2009b. 5929, 5930, 5964
- 15 Edwards, M.: Long-term and regional variability of phytoplankton biomass in the Northeast Atlantic (1960–1995), *ICES J. Mar. Sci.*, 58, 39–49, doi:10.1006/jmsc.2000.0987, 2001. 5943
- Edwards, M. and Richardson, A. J.: Impact of climate change on marine pelagic phenology and trophic mismatch., *Nature*, 430, 881–4, doi:10.1038/nature02808, 2004. 5934
- Edwards, K. F., Thomas, M. K., Klausmeier, C. a., and Litchman, E.: Allometric scaling and taxonomic variation in nutrient utilization traits and maximum growth rate of phytoplankton, *Limnol. Oceanogr.*, 57, 554–566, doi:10.4319/lo.2012.57.2.0554, 2012. 5947
- 20 Eppley, R.: Temperature and phytoplankton growth in the sea, *Fish. Bull.*, 70, 1063–1085, 1972. 5927
- Geider, R. J., MacIntyre, H. L., and Kana, T. M.: A dynamic regulatory model of phytoplanktonic acclimation to light, nutrients, and temperature, *Limnol. Oceanogr.*, 43, 679–694, 1998. 5927, 5950
- Gnanadesikan, A.: Oceanic ventilation and biogeochemical cycling: Understanding the physical mechanisms that produce realistic distributions of tracers and productivity, *Global Biogeochem. Cy.*, 18, GB4010, doi:10.1029/2003GB002097, 2004. 5931
- 30 Gregg, W. W.: Ocean primary production and climate: Global decadal changes, *Geophys. Res. Lett.*, 30, 10–13, doi:10.1029/2003GL016889, 2003. 5943, 5944
- Gregg, W. and Casey, N.: Modeling coccolithophores in the global oceans, *Deep-Sea Res. Pt. II*, 54, 447–477, doi:10.1016/j.dsr2.2006.12.007, 2007. 5926
- Hashioka, T., Vogt, M., Yamanaka, Y., Le Quere, C., Buitenhuis, E., Aita, M. N., Alvain, S., Bopp, L., Hirata, T., Lima, I., Sailley, S., and Doney, S.: Phytoplankton competition during the spring bloom in four Plankton Functional Type Models, *Biogeosciences Discussions*, 9, 18083–18129, doi:10.5194/bgd-9-18083-2012, 2012. 5930, 5935, 5938, 5939
- 5

## PFTs and Export Production 1960–2006

C. Laufkötter et al.

Title Page

Abstract

Introduction

Conclusions

References

Tables

Figures

◀

▶

◀

▶

Back

Close

Full Screen / Esc

Printer-friendly Version

Interactive Discussion



- Head, E. J. H. and Pepin, P.: Spatial and inter-decadal variability in plankton abundance and composition in the Northwest Atlantic (1958–2006), *J. Plankt. Res.*, 32, 1633–1648, doi:10.1093/plankt/fbq090, 2010. 5943
- 10 Hirata, T., Hardman-Mountford, N. J., Brewin, R. J. W., Aiken, J., Barlow, R., Suzuki, K., Isada, T., Howell, E., Hashioka, T., Noguchi-Aita, M., and Yamanaka, Y.: Synoptic relationships between surface Chlorophyll-*a* and diagnostic pigments specific to phytoplankton functional types, *Biogeosciences*, 8, 311–327, doi:10.5194/bg-8-311-2011, 2011. 5926, 5930, 5931, 5948
- 15 Holling, C.: The functional response of predators to prey density and its role in mimicry and population regulation, *Memo. Entomolog. Soc. Canada*, 45, 61 pp., 1965. 5938, 5950
- Iglesias-Rodríguez, M. D.: Representing key phytoplankton functional groups in ocean carbon cycle models: Coccolithophorids, *Global Biogeochem. Cy.*, 16, 1–20, doi:10.1029/2001GB001454, 2002. 5925
- 20 Kahru, M., Kudela, R., Manzano-Sarabia, M., and Mitchell, B. G.: Trends in primary production in the California Current detected with satellite data, *J. Geophys. Res.*, 114, 1–7, doi:10.1029/2008JC004979, 2009. 5943
- Kalnay, E., Kanamitsu, M., Kistler, R., Collins, W., Deaven, D., Gandin, L., Iredell, M., Saha, S., White, G., Woollen, J., Zhu, Y., Chelliah, M., Ebisuzaki, W., Higgins, W., Janowiak, J., Mo, K. C., Ropelewski, C., Wang, J., Leetmaa, A., Reynolds, R., Jenne, R., and Joseph, D.: The NCEP/NCAR 40-year reanalysis project, *Bull. Amer. Meteor. Soc.*, 77, 437–470, 1996. 5929
- 25 Kishi, M., Kashiwai, M., Ware, D., Megrey, B., Eslinger, D., Werner, F., Noguchiaita, M., Azumaya, T., Fujii, M., and Hashimoto, S.: NEMURO – a lower trophic level model for the North Pacific marine ecosystem, *Ecol. Modell.*, 202, 12–25, doi:10.1016/j.ecolmodel.2006.08.021, 2007. 5926
- 30 Klaas, C. and Archer, D. E.: Association of sinking organic matter with various types of mineral ballast in the deep sea: Implications for the rain ratio, *Global Biogeochem. Cy.*, 16, 1116, doi:10.1029/2001GB001765, 2002. 5929, 5941
- Large, W. and Yeager, S.: Diurnal to decadal global forcing for ocean and sea-ice models: the data sets and flux climatologies, 2004. 5930, 5945
- Large, W. G. and Yeager, S. G.: The global climatology of an interannually varying air-sea flux data set, *Clim. Dynam.*, 33, 341–364, doi:10.1007/s00382-008-0441-3, 2009. 5929, 5945

## PFTs and Export Production 1960–2006

C. Laufkötter et al.

Title Page

Abstract

Introduction

Conclusions

References

Tables

Figures



Back

Close

Full Screen / Esc

Printer-friendly Version

Interactive Discussion



- 5 Le Quéré, C., Aumont, O., Monfray, P., and Orr, J.: Propagation of climatic events on ocean stratification, marine biology, and CO<sub>2</sub>: Case studies over the 1979–1999 period, *J. Geophys. Res.*, 108, 3375, doi:10.1029/2001JC000920, 2003. 5936, 5946
- Le Quéré, C., Harrison, S. P., Prentice, I., Buitenhuis, E. T., Aumont, O., Bopp, L., Claustre, H., Da Cunha, L. C., Geider, R., Giraud, X., Klaas, C., Kohfeld, K. E., Legendre, L., Manizza, M., Platt, T., Rivkin, R. B., Sathyendranath, S., Uitz, J., Watson, A. J., and Wolf-Gladrow, D.: Ecosystem dynamics based on plankton functional types for global ocean biogeochemistry models, *Glob. Change Biol.*, 11, 2016–2040, doi:10.1111/j.1365-2486.2005.01004.x, 2005. 5925, 5946
- 10 Levitus, S., Antonov, J. I., Boyer, T. P., Locarnini, R. a., Garcia, H. E., and Mishonov, a. V.: Global ocean heat content 1955–2008 in light of recently revealed instrumentation problems, *Geophys. Res. Lett.*, 36, doi:10.1029/2008GL037155, 2009. 5924
- 15 Mackas, D. L.: Does blending of chlorophyll data bias temporal trend?, *Nature*, 472, E4–5; discussion E8–9, doi:10.1038/nature09951, 2011. 5926, 5942
- Marinov, I., Doney, S. C., and Lima, I. D.: Response of ocean phytoplankton community structure to climate change over the 21st century: partitioning the effects of nutrients, temperature and light, *Biogeosciences*, 7, 3941–3959, doi:10.5194/bg-7-3941-2010, 2010. 5926, 5946
- 20 McClain, C. R., Feldman, G. C., and Hooker, S. B.: An overview of the SeaWiFS project and strategies for producing a climate research quality global ocean bio-optical time series, *Deep-Sea Res. Pt. II*, 51, 5–42, doi:10.1016/j.dsr2.2003.11.001, 2004. 5930
- 25 McQuatters-Gollop, A., Raitsos, D. E., Edwards, M., Pradhan, Y., Mee, L. D., Lavender, S. J., and Attril, M. J.: A long-term chlorophyll data set reveals regime shift in North Sea phytoplankton biomass unconnected to nutrient trends, *Limnol. Oceanogr.*, 52, 635–648, 2007. 5943
- McQuatters-Gollop, A., Reid, P. C., Edwards, M., Burkill, P. H., Castellani, C., Batten, S., Gieskes, W., Beare, D., Bidigare, R. R., Head, E., Johnson, R., Kahru, M., Koslow, J. A., and Pena, A.: Is there a decline in marine phytoplankton?, *Nature*, 472, E6–E7, doi:10.1038/nature09950, 2011. 5926, 5942
- 30 Moore, J., Doney, S., Kleypas, J., Glover, D., and Fung, I.: An intermediate complexity marine ecosystem model for the global domain, *Deep-Sea Res. Pt. II*, 49, 403–462, doi:10.1016/S0967-0645(01)00108-4, 2002. 5927, 5928
- Moore, J. K., Doney, S. C., and Lindsay, K.: Upper ocean ecosystem dynamics and iron cycling in a global three-dimensional model, *Global Biogeochem. Cy.*, 18, 1–21, doi:10.1029/2004GB002220, 2004. 5927, 5952

## PFTs and Export Production 1960–2006

C. Laufkötter et al.

[Title Page](#)
[Abstract](#)
[Introduction](#)
[Conclusions](#)
[References](#)
[Tables](#)
[Figures](#)

[Back](#)
[Close](#)
[Full Screen / Esc](#)
[Printer-friendly Version](#)
[Interactive Discussion](#)


- 5 Moore, K. J. and Abbott, R.: Phytoplankton chlorophyll distributions and primary production in the Southern Ocean, *J. Geophys. Res.*, 105, 28709–28722, 2000. 5945
- Najjar, R. G., Jin, X., Louanchi, F., Aumont, O., Caldeira, K., Doney, S. C., Dutay, J.-C., Follows, M., Gruber, N., Joos, F., Lindsay, K., Maier-Reimer, E., Matear, R. J., Matsumoto, K., Monfray, P., Mouchet, A., Orr, J. C., Plattner, G.-K., Sarmiento, J. L., Schlitzer, R., Slater, R. D., Weirig, M.-F., Yamanaka, Y., and Yool, A.: Impact of circulation on export production, dissolved organic matter, and dissolved oxygen in the ocean: Results from Phase II of the Ocean Carbon-cycle Model Intercomparison Project (OCMIP-2), *Global Biogeochem. Cy.*, 21, doi:10.1029/2006GB002857, 2007. 5931, 5948
- 10 Pelejero, C., Calvo, E., and Hoegh-Guldberg, O.: Paleo-perspectives on ocean acidification, *Trends Ecol. Evolut.*, 25, 332–44, doi:10.1016/j.tree.2010.02.002, 2010. 5925
- 15 Polovina, J. J., Howell, E. a., and Abecassis, M.: Ocean's least productive waters are expanding, *Geophys. Res. Lett.*, 35, 2–6, doi:10.1029/2007GL031745, 2008. 5925
- Pomeroy, L. and Wiebe, W.: Temperature and substrates as interactive limiting factors for marine heterotrophic bacteria, *Aq. Microb. Ecol.*, 23, 187–204, doi:10.3354/ame023187, 2001. 5947
- 20 Raitsos, D. E.: Extending the SeaWiFS chlorophyll data set back 50 years in the Northeast Atlantic, *Geophys. Res. Lett.*, 32, 2–5, doi:10.1029/2005GL022484, 2005. 5943
- Reid, P. C., Edwards, M., Hunt, H. G., and Warner, A. J.: Phytoplankton change in the North Atlantic, *Nature*, 391, 546, 1998. 5943
- 25 Richardson, A. J. and Schoeman, D. S.: Climate impact on plankton ecosystems in the North-east Atlantic., *Science*, 305, 1609–12, doi:10.1126/science.1100958, 2004. 5926
- Riebesell, U., Körtzinger, A., and Oschlies, A.: Sensitivities of marine carbon fluxes to ocean change, *Proc. Natl. Acad. Sci. USA*, 106, 20602–20609, doi:10.1073/pnas.0813291106, 2009. 5947
- 30 Rykaczewski, R. R. and Dunne, J. P.: A measured look at ocean chlorophyll trends, *Nature*, 472, E5–6, doi:10.1038/nature09952, 2011. 5926, 5942
- Saba, V. S., Friedrichs, M. a. M., Carr, M.-E., Antoine, D., Armstrong, R. a., Asanuma, I., Aumont, O., Bates, N. R., Behrenfeld, M. J., Bennington, V., Bopp, L., Bruggeman, J., Buitenhuis, E. T., Church, M. J., Ciotti, A. M., Doney, S. C., Dowell, M., Dunne, J., Dutkiewicz, S., Gregg, W., Hoepffner, N., Hyde, K. J. W., Ishizaka, J., Kameda, T., Karl, D. M., Lima, I., Lomas, M. W., Marra, J., McKinley, G. a., Mélin, F., Moore, J. K., Morel, A., O'Reilly, J., 5 Salihoglu, B., Scardi, M., Smyth, T. J., Tang, S., Tjiputra, J., Uitz, J., Vichi, M., Waters, K.,

## PFTs and Export Production 1960–2006

C. Laufkötter et al.

[Title Page](#)
[Abstract](#)
[Introduction](#)
[Conclusions](#)
[References](#)
[Tables](#)
[Figures](#)
[Back](#)
[Close](#)
[Full Screen / Esc](#)
[Printer-friendly Version](#)
[Interactive Discussion](#)


Westberry, T. K., and Yool, A.: Challenges of modeling depth-integrated marine primary productivity over multiple decades: A case study at BATS and HOT, *Global Biogeochem. Cy.*, 24, GB3020, doi:10.1029/2009GB003655, 2010. 5943

10 Sailley, S., Vogt, M., Doney, S., Aita, M., Bopp, L., Buitenhuis, E., Hashioka, T., Lima, I., Le Quere, C., and Yamanaka, Y.: Comparing food web structures and dynamics across a suite of global marine ecosystem models, submitted, 2013. 5930, 5931, 5935, 5947

Sarmiento, J. L., Slater, R., Barber, R., Bopp, L., Doney, S. C., Hirst, A., Kleypas, J., Matear, R., Mikolajewicz, U., Monfray, P., Soldatov, V., Spall, S., and Stouffer, R.: Response of ocean ecosystems to climate warming, *Global Biogeochem. Cy.*, 18, GB3003, doi:10.1029/2003GB002134, 2004. 5936, 5945

Schlitzer, R.: Carbon export fluxes in the Southern Ocean: Results from inverse modeling and comparison with satellite-based estimates, *Deep-Sea Res. Pt. II*, 49, 1623–1644, doi:10.1016/S0967-0645(02)00004-8, 2002. 5931

20 Smith, T. M., Reynolds, R. W., Peterson, T. C., and Lawrimore, J.: Improvements to NOAA's Historical Merged Land Ocean Surface Temperature Analysis (1880–2006), *J. Climate*, 21, 2283–2296, doi:10.1175/2007JCLI2100.1, 2008. 5935

Sommer, U. and Lengfellner, K.: Climate change and the timing, magnitude, and composition of the phytoplankton spring bloom, *Global Change Biology*, 14, 1199–1208, doi:10.1111/j.1365-2486.2008.01571.x, 2008. 5926

25 Steinacher, M., Joos, F., Frölicher, T. L., Bopp, L., Cadule, P., Cocco, V., Doney, S. C., Gehlen, M., Lindsay, K., Moore, J. K., Schneider, B., and Segschneider, J.: Projected 21st century decrease in marine productivity: a multi-model analysis, *Biogeosciences*, 7, 979–1005, doi:10.5194/bg-7-979-2010, 2010. 5925, 5936, 5945, 5946

30 Vogt, M., Hashioka, T., Le Quéré, C., Alvain, S., Bopp, L., Buitenhuis, E., Doney, S. C., Lima, I., Aita, M., and Yamanaka, Y.: MARine Ecosystem Model Inter-comparison Project (MAREMIP): The representation of ecological niches in different Dynamic Green Ocean Models, in preparation, 2013. 5930, 5931

Volk, T. and Hoffert, M.: Ocean carbon pumps: Analysis of relative strengths and efficiencies in ocean-driven atmospheric CO<sub>2</sub> changes, in: *The Carbon Cycle and Atmospheric CO<sub>2</sub>: Natural Variations Archean to Present*, Geophys. Monogr. Ser., vol. 32, edited by: Sundquist, E. and Broecker, W., 99–110, American Geophysical Union, Washington, DC, 99–110 doi:10.1029/GM032p0099, 1985. 5925

**PFTs and Export  
Production  
1960–2006**

C. Laufkötter et al.

[Title Page](#)[Abstract](#)[Introduction](#)[Conclusions](#)[References](#)[Tables](#)[Figures](#)[Back](#)[Close](#)[Full Screen / Esc](#)[Printer-friendly Version](#)[Interactive Discussion](#)

- 1035 Wang, S. and Moore, J. K.: Variability of primary production and air-sea CO<sub>2</sub> flux in the Southern  
Ocean, *Global Biogeochem. Cy.*, 26, GB1008, doi:10.1029/2010GB003981, 2012. 5945
- Weber, T. and Deutsch, C.: Oceanic nitrogen reservoir regulated by plankton diversity and  
ocean circulation, *Nature*, 489, 419–422, doi:10.1038/nature11357, 2012. 5947
- Yeager, S. G., Shields, C. a., Large, W. G., and Hack, J. J.: The Low-Resolution CCSM3, *J.*  
1040 *Climate*, 19, 2545–2566, doi:10.1175/JCLI3744.1, 2006. 5927
- Zwiers, F. W. and von Storch, H.: Taking serial correlation into account in tests of the mean, *J.*  
*Climate*, 8, 336–351, 1995. 5931

**Table 1.** Parameters of the ecosystem model BEC. Bold numbers in brackets denote values that have been used in the version of Doney et al. (2009b).

Parameter	Value	Units	Definition
$\mu_{\max}$	3.0	$\text{d}^{-1}$	max. phyto. C-specific growth rate at $T_{\text{ref}}$
$q_{10}$	2		temperature dependence factor
$T_{\text{ref}}$	30	$^{\circ}\text{C}$	reference temperature
$T_{\text{K}0}$	273.16	K	zero point for Celsius
$\alpha$	0.3 <b>(0.25)</b>	$\frac{\text{mmol C m}^2}{(\text{mg Chl W d})^{-1}}$	initial slope of P-I curve
$K_{\text{sp}}^{\text{PO}_4}$	$3.125 \times 10^{-4}$	$\text{mmol PO}_4 \text{ m}^{-3}$	small phyto. $\text{PO}_4$ half saturation coefficient
$K_{\text{sp}}^{\text{NO}_3}$	0.5	$\text{mmol N m}^{-3}$	small phyto. $\text{NO}_3$ half saturation coefficient
$K_{\text{sp}}^{\text{NH}_4}$	0.005	$\text{mmol N m}^{-3}$	small phyto. $\text{NH}_4$ half saturation coefficient
$K_{\text{sp}}^{\text{Fe}}$	$6 \times 10^{-5}$	$\text{mmol Fe m}^{-3}$	small phyto. Fe half saturation coefficient
$K_{\text{diat}}^{\text{PO}_4}$	0.005	$\text{mmol PO}_4 \text{ m}^{-3}$	diatom $\text{PO}_4$ half saturation coefficient
$K_{\text{diat}}^{\text{NO}_3}$	2.5	$\text{mmol N m}^{-3}$	diatom $\text{NO}_3$ half saturation coefficient
$K_{\text{diat}}^{\text{NH}_4}$	0.08 <b>(0.1)</b>	$\text{mmol N m}^{-3}$	diatom $\text{NH}_4$ half saturation coefficient
$K_{\text{diat}}^{\text{Fe}}$	$1.5 \times 10^{-4}$	$\text{mmol Fe m}^{-3}$	diatom Fe half saturation coefficient
$K_{\text{diat}}^{\text{SiO}_3}$	1.0	$\text{mmol SiO}_3 \text{ m}^{-3}$	diatom Si half saturation coefficient
$i_z$	0.3		zooplankton ingestion coefficient (non dim)
$a_{\text{sp}}^{\max}$	0.2	$\text{d}^{-1}$	max. aggregation rate for small phyto.
$a_{\text{diat}}^{\max}$	0.2	$\text{d}^{-1}$	max. aggregation rate for diatoms
$a_{\text{diat}}^{\min}$	0.01	$\text{d}^{-1}$	min. aggregation rate for diatoms
$e_{\text{sp}}^{\text{POC}}$	0.18 <b>(0.22)</b>	$(\text{mmol C})^{-1}$	small phyto. grazing factor
$u_{\text{sp}}^{\max}$	2.75	$\text{d}^{-1}$	max. zoo. growth rate on small phyto. at $T_{\text{ref}}$
$u_{\text{diat}}^{\max}$	2.07 <b>(2.0)</b>	$\text{d}^{-1}$	max. zoo. growth rate on diatoms at $T_{\text{ref}}$
$g$	1.05	$\text{mmol C m}^{-3}$	zoo. grazing coefficient
$f_z^{\text{small}}$	1		scaling factor for grazing on small
$f_z^{\text{diat}}$	0.81		scaling factor for grazing on diatoms

## PFTs and Export Production 1960–2006

C. Laufkötter et al.

Title Page

Abstract

Introduction

Conclusions

References

Tables

Figures

◀

▶

◀

▶

Back

Close

Full Screen / Esc

Printer-friendly Version

Interactive Discussion



PFTs and Export  
Production  
1960–2006

C. Laufkötter et al.

Table 1. Continued.

Parameter	Value	Units	Definition
$f_{\text{graz}}^{\text{CaCO}_3, \text{POC}}$	0.4		min. proportionality between $Q_{\text{small}}^{\text{CaCO}_3}$ and grazing losses to POC
$f_{\text{graz}}^{\text{small, POC}}$	0.22 (0.24)		upper limit on fraction of grazing on small phyto. routed to POC
$f_{\text{sp, DOC}}^{\text{graz}}$	0.34		fraction of small phyto. grazing to DOC
$f_{\text{sp, DIC}}^{\text{graz}}$	$1 - (i_z + f_{\text{graz}}^{\text{sp, DOC}})$		fraction of grazing on small phyto. routed to DIC
$f_z^{\text{diat}}$	0.81		scaling factor for grazing on diatoms
$f_{\text{graz}}^{\text{diat, POC}}$	0.26		fraction of diatom grazing routed to POC
$f_{\text{graz}}^{\text{diat, DOC}}$	0.13		fraction of diatom grazing routed to DOC
$f_{\text{graz}}^{\text{diat, DIC}}$	$1 - (i_z + f_{\text{graz}}^{\text{diat, POC}} + f_{\text{graz}}^{\text{diat, DOC}})$		fraction of diatom grazing routed to DIC
$P_{\text{small}, P_{\text{diat}}}$	0.009	$(\text{mmol C})^{-1} \text{m}^3 \text{d}^{-1}$	small phyto/diatom quadratic mortality rate
$\lambda_{\text{POC}}$	13000	cm	remineralization length scale for “soft” particulate POC
$\lambda_{\text{PCaCO}_3}$	60000	cm	remineralization length scale for “soft” particulate $\text{CaCO}_3$
$\lambda_{\text{PSiO}_3}$	2200	cm	remineralization length scale for “soft” particulate $\text{SiO}_3$
$\lambda_{\text{dust}}$	60000	cm	remineralization length scale for “soft” dust
$\lambda_{\text{hard}}$	$4 \times 10^6$	cm	remineralization length scale for all “hard” particulate subclasses
$\omega_{\text{PCaCO}_3}$	$0.07 \times \frac{M_{\text{CaCO}_3}}{M_{\text{POC}}}$		qualitative associated POC/ $\text{CaCO}_3$ mass ratio for particulate matter
$\omega_{\text{PSiO}_3}$	$0.035 \times \frac{M_{\text{SiO}_3}}{M_{\text{POC}}}$		qualitative associated POC/ $\text{SiO}_3$ mass ratio for particulate matter
$\omega_{\text{dust}}$	$0.07 \times \frac{M_{\text{dust}}}{M_{\text{POC}}}$		qualitative associated POC/dust mass ratio for particulate matter
$f_{\text{PCaCO}_3}^{\text{hard}}$	0.55		fraction of particulate $\text{CaCO}_3$ production routed to “hard” subclass
$f_{\text{PSiO}_3}^{\text{hard}}$	0.37		fraction of particulate $\text{SiO}_3$ production routed to “hard” subclass
$\text{CaCO}_3^{\text{T}}, \text{thres1}$	1.0	$^{\circ}\text{C}$	temperature threshold for calcification
$\text{CaCO}_3^{\text{T}}, \text{thres2}$	-2.0	$^{\circ}\text{C}$	temperature threshold for calcification
$M_{\text{POC}}$	12.01	g	POC molar mass
$M_{\text{CaCO}_3}$	100.09	g	$\text{CaCO}_3$ molar mass
$M_{\text{SiO}_3}$	60.08	g	$\text{SiO}_3$ molar mass
$M_{\text{dust}}$	$1 \times 10^9$	g	dust molar mass
$Q_{\text{diat, opt}}^{\text{Si}}$	0.137		initial diatom Si : C ratio
$Q_{\text{diat, coeff}}^{\text{Si}}$	2.5		

Title Page

Abstract

Introduction

Conclusions

References

Tables

Figures

◀

▶

◀

▶

Back

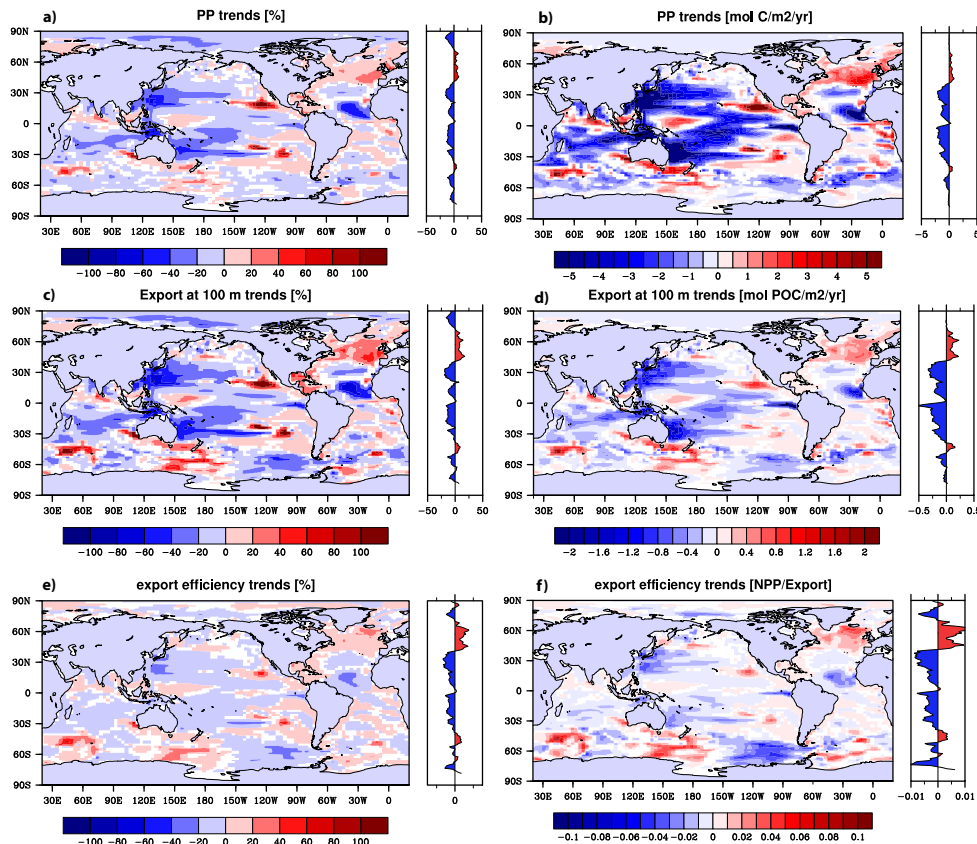
Close

Full Screen / Esc

Printer-friendly Version

Interactive Discussion



[Title Page](#)
[Abstract](#)
[Introduction](#)
[Conclusions](#)
[References](#)
[Tables](#)
[Figures](#)
[Back](#)
[Close](#)
[Full Screen / Esc](#)
[Printer-friendly Version](#)
[Interactive Discussion](#)


**Fig. 1.** Simulated changes in primary production **(a)** and **(b)**, particle export production **(c)** and **(d)** and export efficiency **(e)** and **(f)** from 1960–2006. Export efficiency is the fraction of primary production that is exported through 100 m, calculated by dividing the export at 100 m by integrated primary production above 100 m. Trends have been calculated for each grid cell with linear regression. Insignificant trends have been set to zero ( $\alpha = 0.5$ ).

## PFTs and Export Production 1960–2006

C. Laufkötter et al.

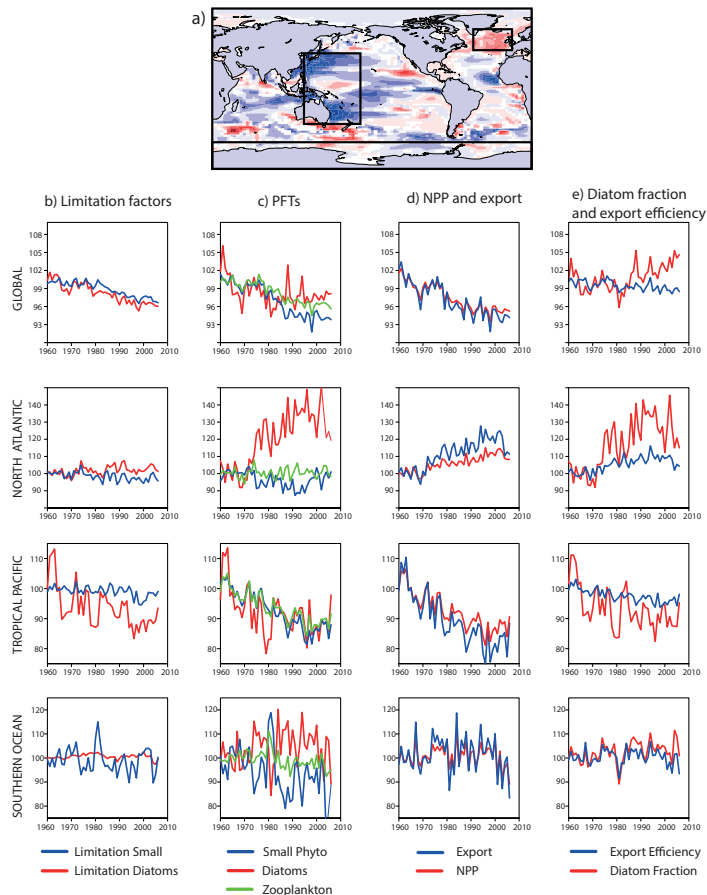


**Fig. 2.** Time series in percent for selected regions **(a)** for the product of light and nutrient limitation **(b)**, PFTs **(c)**, Export and NPP **(d)**, and Export efficiency and diatom fraction **(e)** from 1960–2006.

[Title Page](#)
[Abstract](#)
[Introduction](#)
[Conclusions](#)
[References](#)
[Tables](#)
[Figures](#)
[Back](#)
[Close](#)
[Full Screen / Esc](#)
[Printer-friendly Version](#)
[Interactive Discussion](#)

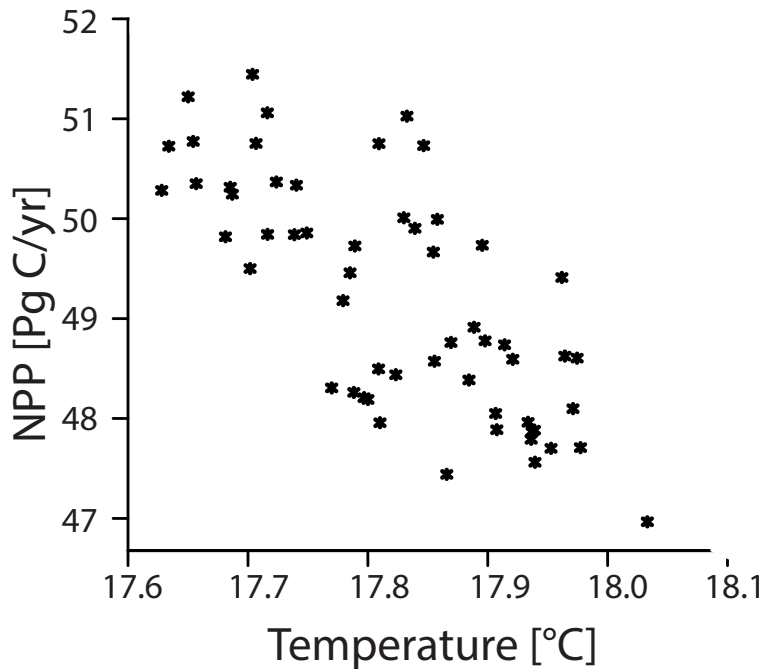


**Fig. 3.** Annual NPP [ $\text{Pg C yr}^{-1}$ ] as a function of changes in mean annual SST [ $^{\circ}\text{C}$ ].

## BGD

10, 5923–5975, 2013

### PFTs and Export Production 1960–2006

C. Laufkötter et al.

Title Page

Abstract

Introduction

Conclusions

References

Tables

Figures



Back

Close

Full Screen / Esc

Printer-friendly Version

Interactive Discussion



PFTs and Export  
Production  
1960–2006

C. Laufkötter et al.

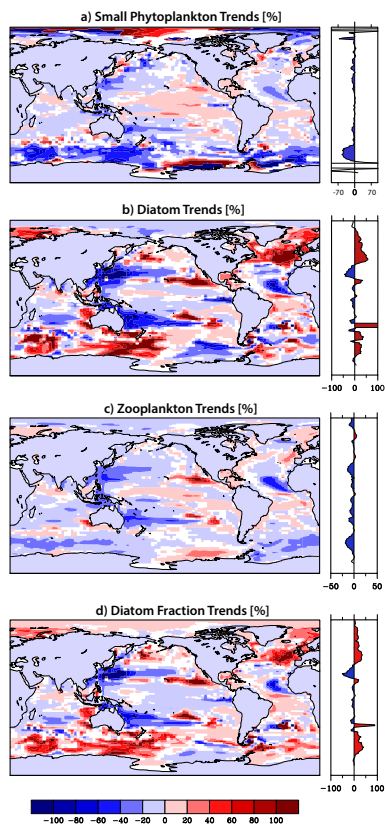


**Fig. 4.** Simulated percental changes in **(a)** small phytoplankton NPP and **(b)** diatom NPP, **(c)** zooplankton biomass and **(d)** resulting changes in diatom fraction.

[Title Page](#)[Abstract](#)[Introduction](#)[Conclusions](#)[References](#)[Tables](#)[Figures](#)[◀](#)[▶](#)[◀](#)[▶](#)[Back](#)[Close](#)[Full Screen / Esc](#)[Printer-friendly Version](#)[Interactive Discussion](#)

## PFTs and Export Production 1960–2006

C. Laufkötter et al.

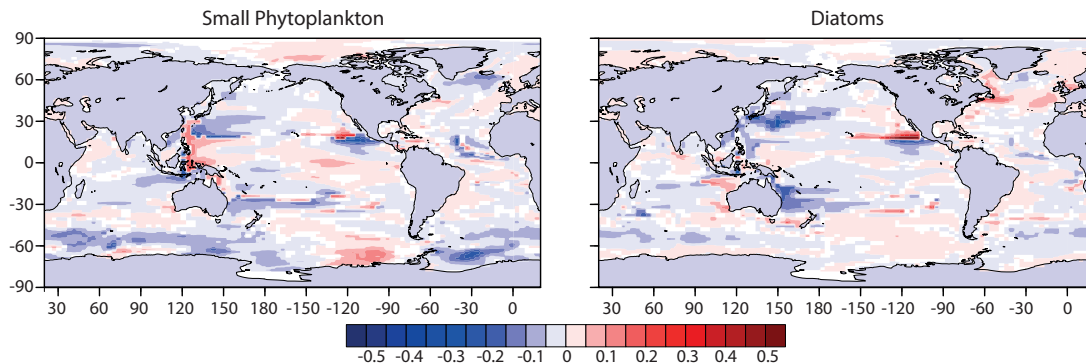


**Fig. 5.** Changes in the product of light and nutrient limitation for diatoms and small phytoplankton

[Title Page](#)[Abstract](#)[Introduction](#)[Conclusions](#)[References](#)[Tables](#)[Figures](#)[Back](#)[Close](#)[Full Screen / Esc](#)[Printer-friendly Version](#)[Interactive Discussion](#)

## PFTs and Export Production 1960–2006

C. Laufkötter et al.

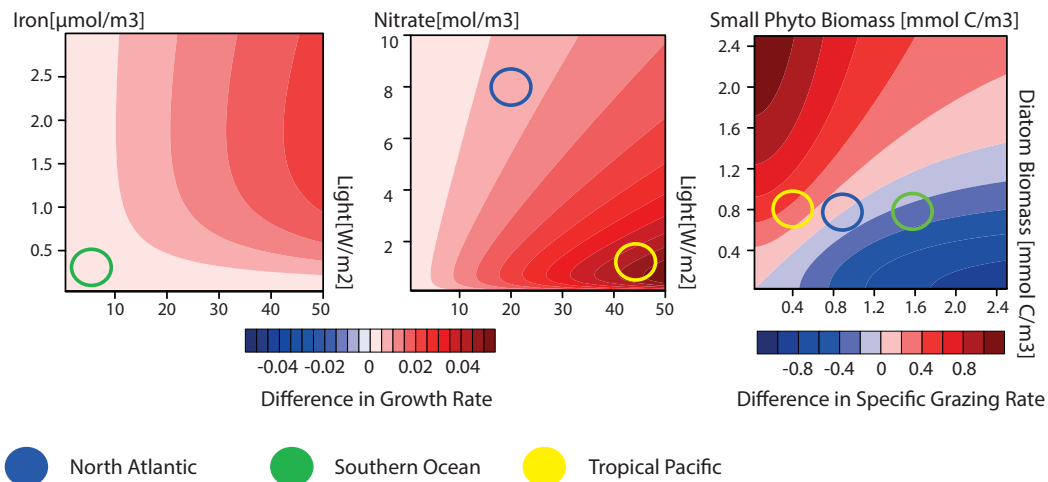


**Fig. 6.** (a) (Small Phytoplankton growth rate – diatom growth rate) at different nitrate, iron and light values. Typical values for regions discussed in the text are marked with coloured circles. The Southern Ocean is mainly iron-limited region, while the subtropical gyres and the North Atlantic are mainly nitrate-limited. (b) (Small phytoplankton grazing rate – diatom grazing rate) at different phytoplankton biomass levels and constant temperature.

## PFTs and Export Production 1960–2006

C. Laufkötter et al.

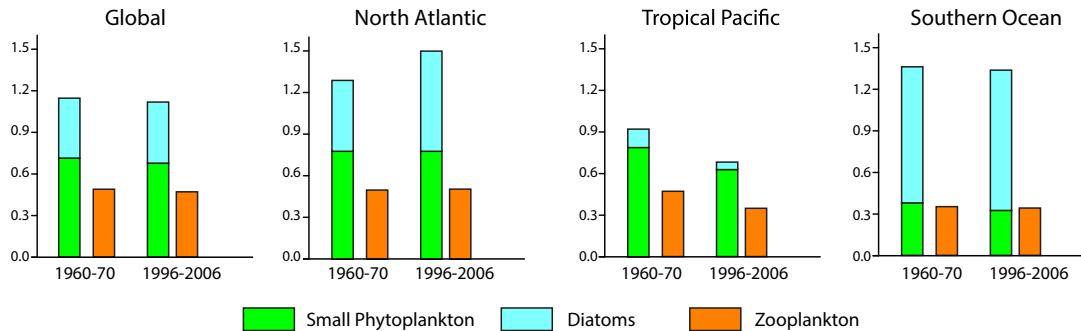


**Fig. 7.** Biomass structure of phytoplankton types and zooplankton at different regions. The ratio is influenced by temperature, with higher temperatures leading to higher zooplankton quota. Moreover diatoms can sustain a lower zooplankton fraction as the zooplankton growth rate is lower when feeding on diatoms.

Title Page

Abstract

Introduction

Conclusions

References

Tables

Figures

◀

▶

◀

▶

Back

Close

Full Screen / Esc

Printer-friendly Version

Interactive Discussion



## PFTs and Export Production 1960–2006

C. Laufkötter et al.

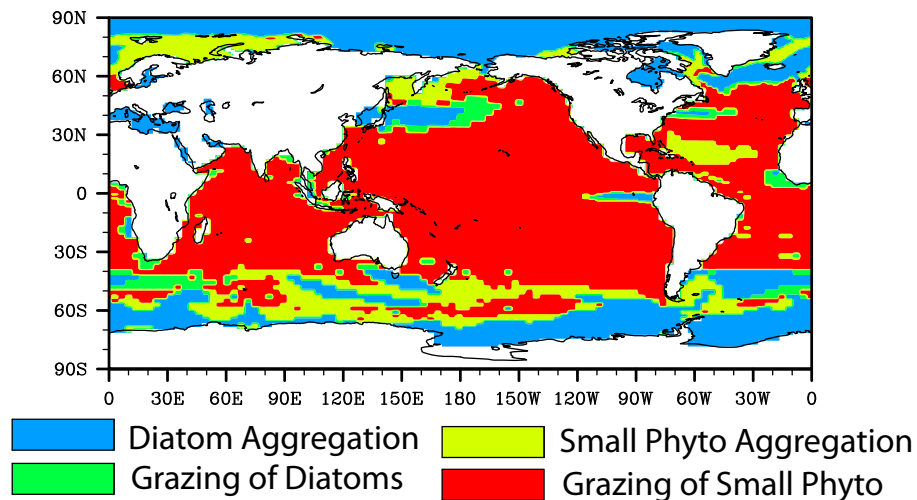


**Fig. 8.** Particle production mechanism which produces the strongest flux of sinking particles on average over the study period. The particle production mechanisms in the BEC are aggregation by diatoms (blue) or small phytoplankton (yellow) and grazing on diatoms (green) or on small phytoplankton (red).

Title Page

Abstract

Introduction

Conclusions

References

Tables

Figures

◀

▶

◀

▶

Back

Close

Full Screen / Esc

Printer-friendly Version

Interactive Discussion



## PFTs and Export Production 1960–2006

C. Laufkötter et al.

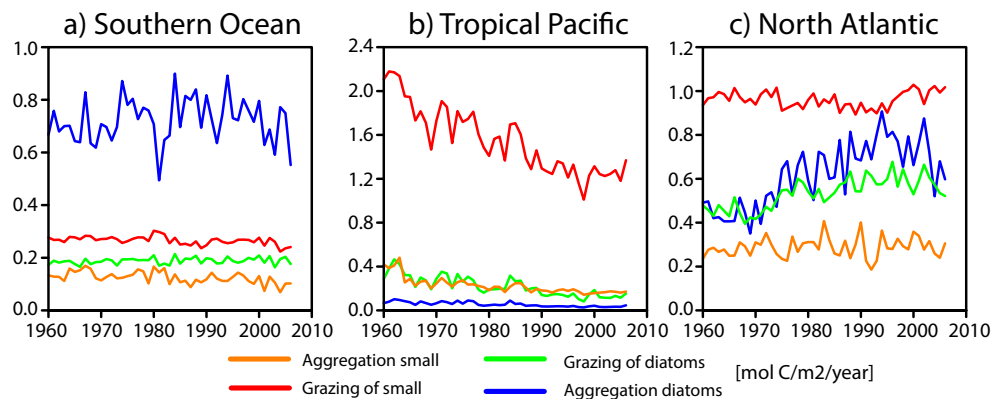


**Fig. 9.** Trends of particle production mechanisms in  $\text{mol C m}^{-2} \text{yr}^{-1}$  for **(a)** the Southern Ocean, **(b)** Tropical Pacific and **(c)** North Atlantic over the simulation period (1960–2006).

Title Page

Abstract

Introduction

Conclusions

References

Tables

Figures

◀

▶

◀

▶

Back

Close

Full Screen / Esc

Printer-friendly Version

Interactive Discussion



## PFTs and Export Production 1960–2006

C. Laufkötter et al.

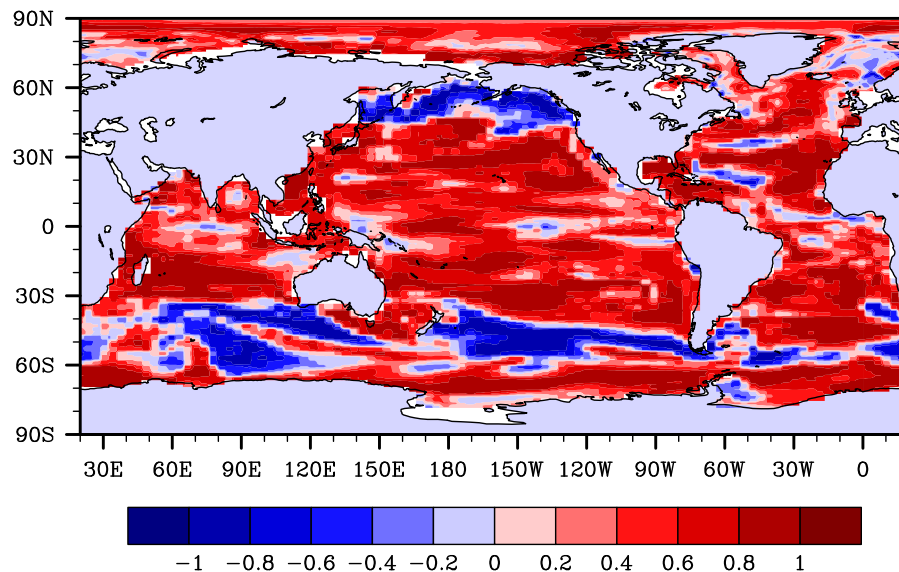


**Fig. 10.** Spearman correlation of diatom fraction with export efficiency at each grid cell. Trends have been removed from the timeseries before calculation. Significance has been tested at significance level  $\alpha = 0.1$ .

[Title Page](#)[Abstract](#)[Introduction](#)[Conclusions](#)[References](#)[Tables](#)[Figures](#)[Back](#)[Close](#)[Full Screen / Esc](#)[Printer-friendly Version](#)[Interactive Discussion](#)